Materials and Devices
An International Scientific Journal
OPEN ACCESS
Freely Accessible Scientific Papers.
CA-IP
Managed by scientists for Science - http://co-ac.com

Article type: A-Regular research paper

Investigation of metallacages for cisplatin encapsulation using Density Functional Theory

S. Y. Ugurlu (1*), R. Enisoglu (2)

(1) School of Computer Science, University of Birmingham, Edgbaston, Birmingham, B15 2TT, United Kingdom, s.yavuz.ugurlu@gmail.com
(2) School of Science and Technology, City St George's, University of London, Northampton Square, London, EC1V 0HB, ramazan.enisoglu@city.ac.uk

***Corresponding author: s.yavuz.ugurlu@gmail.com**

RECEIVED: 21 October 2024 / REVISED: 27 November 2024 / ACCEPTED: 10 December 2024

Abstract: Cancer is highly complex, including cross-talks between signalling pathways and multiple genes. Fortunately, successful anti-cancer drugs, such as cisplatin, are promising to treat cancer. Despite its clinical success, cisplatin presents several issues, including neurotoxicity, ototoxicity, nephrotoxicity, and drug resistance. New supramolecular drug delivery systems can fix these problems with the effective cancer drug cisplatin. This research aims to optimise novel supramolecular drug delivery systems—metallacage (M2L4 (M = metal, L = ligand)—that can be used to encapsulate cisplatin to protect it from metabolism. Specifically, we investigated the shape and stability of ten metallacages using different metals: Pt2+, Pd2+, Ni2+, Cu2+ and Au3+ using Density Functional Theory (DFT) methods to encapsulate one or two cisplatin molecules. Therefore, we utilised WebMo to run PBE0 and Hartree Fock theories, using LanL2DZ as a basis set. The results demonstrate that PBE0/LanL2DZ is the best method to describe the cages. The results show that Endo-N Ni2L4 and Endo-N Cu2L4 cages are the best ways to encapsulate cisplatins one and two. Endo-C Pt2L4 and Endo-C Au2L4, on the other hand, are the least suitable systems for encapsulating cisplatins. Furthermore, Endo-C cages are farther from ground-state energy because they are higher than Endo-N cages. Therefore, Endo-N cages are superior to Endo-C cages for the encapsulation of cisplatin.

Keywords: Cancer, cisplatin, metallacage, supramolecular, DFT.

Cite this article: S. Y. Ugurlu, R. Enisoglu, OAJ Materials and Devices, Vol 8, 0412 (2024) - DOI: 10.23647/ca.md20240412

1. Introduction

The metals used in medicine were noticed after their successful works, such as sodium vanadate used in diabetic patients, and gold benefitted by reducing inflammation [1]. Cis-diamminedichloridoplatinum(II) (cisplatin) was discovered in the late 1960s as a cancer treatment due to its cytotoxic effects. [2]. The Food and Drug Administration (FDA) approved it in 1978 and has since used it to treat several cancers, particularly those of the bladder, testicles, and ovaries. The rate of accomplished treatment with cis-platin is over 90% for patients having testicular cancer [3, 4]. However, cisplatin has been suffering from limitations, such as neurotoxicity, ototoxicity, and nephrotoxicity, which results in painful treatment and restricts the usage of cisplatin [3, 4, 5, 6, 7, 8, 9, 10, 11, 12].

Reducing the limitations of cisplatin, such as neurotoxicity, ototoxicity, and nephrotoxicity, is becoming more vital because of the around 90% success rate of cisplatin in cancer treatment [3, 4, 6, 7, 8, 9]. The other limitation is drug resistance against cisplatin in cancer treatment [10, 11, 12]. One example is that ovarian cancer cells become resistant to cisplatin when they lose signal-regulated kinase (ERK) [8]. Moreover, there are several things that make drugs less effective: HSA (human serum albumins), influx and efflux transporters (drugs getting into cancer cells), DNA repair mechanisms (base excision repair, nucleotide repair, and mismatch repair), and high levels of glutathione [8, 13, 14]. Consequently, cisplatin has problems like neurotoxicity, ototoxicity, and nephrotoxicity [15]. However, new methods, such as supramolecular coordination complexes (SCCs) [15], can address these issues by making drugs less effective [3, 4, 6, 7, 8, 9].

SCCs, such as metallacages, can be easily synthesised and modified in various geometries and redox states, allowing their features to be altered. This flexibility helps overcome the limitations of cisplatin [16, 17, 18, 19]. SCCs are highly versatile and can form various architectures, making them promising candidates for applications such as drug delivery [20, 21]. SCCs have shown promise for encasing cisplatin, a commonly used chemotherapy drug because they can make clear, protective spaces that make the drug more stable and help it reach the right place [20, 21]. They have many benefits, including voids for drug delivery, good electrical conductivity and high charge mobility, a very low density, complex unit cells, many van der Waals interactions, easy-to-achieve porosity, and thermal stability [22]. Because of these advantages, metallacages, a type of SCC, are particularly useful for encapsulating drugs to combat toxicity and drug resistance [23, 24].

The metallacages have many advantages, including high symmetry, ease of synthesis, a simple modification that lowers toxicity, and the ability to overcome drug resistance [24, 25, 26, 27, 26]. Additionally, the most commonly used synthesis methods for metallacages are edge- or face-directed [17]. They are symbolised MxLy (M=metal, L=ligand, and x and y are their numbers); for example, Pd12L24 directed-type metallacages were synthesised [28]. The edge-directed synthesis method binds a guest to a Pd2L4 cage, utilising the H-bond, steric interaction, van der Waals, and Coulomb interactions between them [29]. In addition, the metallacages are appropriate for encapsulating anions, cations, and neutral organic molecules [30]. Therefore, these kinds of metallacages can encapsulate cisplatin to overcome its drawbacks, including toxicity, and achieve drug resistance [3, 4, 6, 7, 8, 9].

Computational methods can test cisplatin encapsulation to overcome its limitations, such as toxicity and drug resistance. Consequently, we used DFT simulations to investigate the stability of the metallacages and their cisplatin encapsulation performance. Exo-functionalized Pd2L4 (L=ligand = 2,6-bis(pyridine-3-ylethynyl)pyridine) cages have already been synthesised and characterised, so the research originated from them [31, 32]. Ex vivo studies have proven that Pd L cage encapsulation for cisplatin reduces the cytotoxic effect of the drug [31]. Therefore, finding cages that are better than Pd2L4 can improve cisplatin delivery further. As a result, ten different M2L4 cages have been investigated consisting of varying transition metals, namely Pt2+, Pd2+, Ni2+, Cu2+, and Au3+, using WebMo [33] to encapsulate one and/or two cis-platin molecules. Consequently, the candidate metallacages were indicated after the investigation of several structures.

2. Materials and Methods

Density Functional Theory (DFT) is an essential part of computational chemistry because it lets us study the electronic structure of molecular systems [34]. It is vital to study metallacages and how they might be used to hold therapeutic substances like cisplatin [31, 32]. Therefore, we utilised DFT to model and analyse cisplatin encapsulation within different metallacages, providing insights into the underlying mechanisms and potential applications in drug delivery.

DFT has been utilised in two critical stages of the computational analysis: (i) Energy minimisation, where the goal is to find the lowest possible energy configuration of the system by adjusting atomic positions [35, 36, 37], and (ii) Geometry optimisation, which involves refining the molecular structure to achieve equilibrium geometry where forces on the atoms are minimised [38, 39].

2.1 Energy minimisation

A fundamental computational technique known as energy minimisation reduces the potential energy of a molecular system to find its most stable configuration [36]. This process involves adjusting the positions of atoms to achieve a conformation where the system's total energy is at a minimum, indicating that the structure is in a stable and energetically favourable state [35, 36, 37]. Energy minimisation is crucial in studying metallacages as it provides a baseline for assessing their stability and suitability for various applications. For cisplatin encapsulation, minimising the energy of the metallacage helps ensure that the structure can effectively stabilise the drug molecule within its framework for safe drug delivery.

2.2 Geometry optimisation

Geometry optimisation is a crucial computational process to refine the structural arrangement of molecules and materials to their lowest energy configuration [38, 39, 40]. This technique involves adjusting the positions of atoms within a structure to minimise its total energy, ensuring that the system achieves a stable and energetically favourable state [38, 39, 41]. Geometry optimisation precisely determines the optimal arrangement of atoms, aiding in evaluating the metal's stability and potential reactivity. Geometry optimisation makes creating effective and reliable carriers for cisplatin and other therapeutic agents easier. An example of energy convergence in geometry optimisation for an empty Endo-C Au2L4 cage is shown in Figure 1.

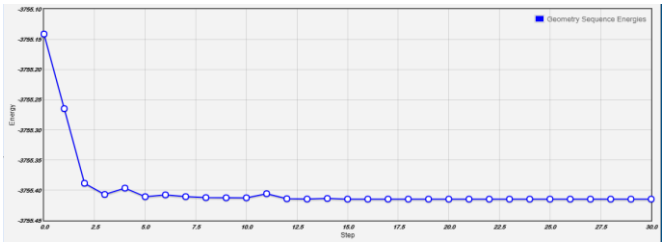

Figure 1: Energy convergence for the empty Endo-C Au2L4 cage during geometry optimisation.

The y-axis represents the system's energy in Hartree, while the x-axis denotes the optimisation steps. The blue line with circular markers shows the energy values at each optimisation step. Initially, there is a significant drop in energy, indicating rapid convergence towards a more stable geometry. As the optimisation proceeds, the energy values stabilise, demonstrating that the system has reached a minimum energy configuration. This convergence behaviour is crucial for verifying that the geometry optimisation process has successfully identified the lowest energy structure for the cage. The stable energy at the final steps confirms the reliability of the optimised geometry for further analysis.

It is crucial to tune the parameters carefully to achieve success in energy minimisation and geometry optimisation. The following section outlines the computational methods employed, detailing the specific software, theories, basis sets, and protocols used.

2.3 Parameters used in energy minimisation and geometry optimisation

For the energy minimisation and geometry optimisation processes, we employed Gaussian 09 software, a widely recognised tool for electronic structure calculations [42, 43, 44]. The Hartree-

Fock theory was used as a starting point for the first energy calculations. It gave a rough idea of how electrons interact [45, 46, 47]. To enhance accuracy, we utilised the Perdew-Burke-Ernzerhof (PBE) functional and its hybrid variant, PBE0, which offer improved performance in describing electron correlation effects [48, 49, 50]. Additionally, we employed the LanL2DZ basis set [51, 52], which is well-suited for accurately representing the electron distribution and facilitating effective optimisation of the molecular geometry of metallacage to encapsulate cisplatin.

Gaussian 9 software

Gaussian, a software package, is coded in Fortran, a programming language for numeric computation and scientific computing [42, 43, 44]. It can be used to calculate computational calculations and solve the Schrodinger equation [53]. It can also predict reactions, bound and reaction energies, IR, NMR, Raman, UV, reaction pathways, and encapsulation of drugs, such as cisplatin [54, 55].

Hartree-Fock Theory

The Hartree-Fock (HF) method is the most straightforward wave function-based approach because it is fundamentally based on a single-particle picture [61]. The method determines the wave function by assuming that each electron occupies an independent orbital and interacts with an averaged field that all other electrons create. However, while HF considers interactions between electrons, it does not consider correlations between electrons, which can lead to errors in systems where these correlations are essential [62]. An atom-centred Gaussian basis set typically solves the Hartree-Fock equations, determining the accuracy of the energy calculations [63]. A fundamental limitation of HF is its inadequacy for problems requiring multiple determinants, such as bond dissociation, where electron correlation plays a crucial role [64]. The Hartree-Fock limit ultimately constrains the method, limiting the potential accuracy achievable with an infinite number of primitives, even though increasing the number of Gaussian primitives can lower the energy [64].

DFT is often better than ab initio methods like HF for systems involving transition metals because it can handle more significant and more complicated structures, like those found in DNA [65]. Therefore, researchers have chosen to investigate cisplatin encapsulation using HF.

PBE and PBE0 Theory

The Perdew–Burke-Ernzerhof (PBE) functional is an approximation used for the exchange-correlation energy in DFT and belongs to the Generalised Gradient Approximation (GGA) family [48]. Though widely used, PBE has limitations, particularly in accurately determining total atomic energies and thermochemical properties [66]. For instance, tests on the PBE function revealed that its performance is comparable to that of BP86, revPBE, and RPBE for simple systems like Na2+. However, we observed significant errors, particularly in transition metal calculations [67]. Consequently, PBE has been experiencing limited performance.

In conclusion, while the PBE functional is a widely used theoretical framework, it has notable limitations in thermochemical measurements, particularly for transition metals [72]. Some of these problems are that it is not always possible to predict thermochemical data correctly, and the local and semi-local approximations used in DFT can lead to errors. To address these issues, hybrid functionals are crucial as they mitigate the drawbacks inherent in traditional DFT methods. When comparing these, PBE0 usually gives better results than PBE because it uses Hartree-Fock exchange, which improves accuracy while keeping the efficiency of computation [49]. Thus, while PBE is a valuable tool, applications requiring higher precision, such as the investigation of complex systems like cisplatin encapsulation, prefer PBE0.

LanL2DZ, as a basis set

Accurate representation of transition metals is crucial for various applications, including drug delivery, advanced material design in biomedical fields, drug discovery and development, and catalytic processes [51]. Transition metals present challenges in accurately describing relativistic effects, outer electrons, low-lying electronic configurations, and the electron relationships in occupied d-orbitals [51]. The LanL2DZ basis set, developed by Hay and Wadt, is a widely used effective core potential (ECP) basis set to address these challenges. It employs pseudo-orbitals with Gaussian functions to efficiently model these complex systems [73, 52].

In conclusion, the LanL2DZ basis set has proven to be a valuable tool in DFT simulations for studying cisplatin encapsulation within metallacages. Its development as an Effective Core Potential (ECP) basis set allows for efficient modelling of transition metals while addressing relativistic effects in deep core electrons [65]. Despite its limitations, such as the absence of polarisation and diffuse functions, LanL2DZ offers a practical balance between computational efficiency and accuracy. Its ability to do this makes it perfect for studying how cisplatin is enclosed, giving us essential information about the stability and interactions in metallacage systems. LanL2DZ's use shows how well it makes complex simulations possible, which is a big part of understanding and improving metallacage-based drug delivery systems.

2.4 Experimental Methodology Setup

Gaussian 09 software, accessible via the WebMo server interface, conducts all encapsulation studies using DFT. This method is chosen to evaluate the performance and encapsulation capabilities of the metallacages. The research aims to elucidate the mechanism behind the release of cytotoxic agents from these cages.

For these simulations, Hartree-Fock (HF), Perdew-Burke-Ernzerhof (PBE), and PBE0 functions are implemented within Gaussian 09. The LanL2DZ basis set is selected for suitability for modelling transition metal systems.

The computational time is set to 48 hours to ensure convergence of results, with a 72-hour limit set for geometry optimisation of cages encapsulating two cisplatin molecules. Once the energy results do not converge within the specified time, the simulation is repeated until either convergence is achieved, the cage structure deteriorates, or the cisplatin is released. Therefore, the structure is at least ten times repeated to find the energy convergence. Once there is no energy convergence after a ten-time run, the results are labelled as" fail."

2.5 Metallacages under investigation

Energy minimisation and geometry optimisation are used to test the performance of several cages using computational and theoretical chemistry. The cages are labelled according to the centre of metals, such as Pd2+, in Figure 2. The other enclosures are formed using Pd2+, Pt2+, Ni2+, Cu2+, and Au3+. In addition, after here, when "X" becomes "C" in Figure 2, the structure is called an Endo-C cage, as well as when "X" turns into "N", the structure is named an Endo-N cage, and "R" is always H in the research. In short, there are ten different cages, four possibilities from metals and two possibilities from X (H and N) (Figure 2). Also, these ten different cages have been tested to encapsulate one and two molecules of cisplatin.

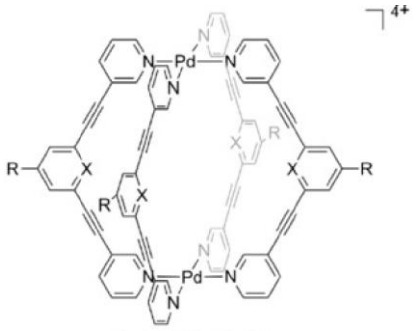

Figure 2: Schematic Representation of a Palladium(II)-Based Metallacage for Cisplatin Encapsulation [97]

The figure depicts a metallacage structure, where palladium (II) ions (Pd) coordinate with nitrogen atoms (N) from bipyridine ligands. Multiple aromatic rings (R groups) and alkyne linkers (X)

design the cage to create a rigid, well-defined framework. The metallacage forms a hexagonal geometry with two palladium centres connected by nitrogen donors, which help stabilise the overall structure. This metallacage is optimised to encapsulate small molecules like cisplatin, providing a potential vehicle for drug delivery. The illustration highlights the spatial arrangement of the ligands and metal centres, emphasising the potential binding sites for guest molecules within the cage's interior. The positive charge (4+) indicates the overall charge of the metallacage in its fully assembled form.

7.2 The distances for Endo-C Cage

To investigate the metallacages, we have calculated two key structural parameters: the distance between the metal centres on the top and bottom of the cage and the distance between the carbon atoms at the equatorial centre (Figure 3). These measurements provide insight into the overall geometry and symmetry of the metallacages, which are crucial for understanding their stability and potential efficacy in applications such as cisplatin encapsulation.

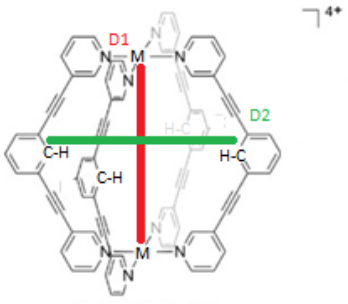

Figure 3: Distance between two metal ions and the C atoms on the side of the structure

Top-view schematic representation of a metallacage structure, highlighting the critical distances D1 (red) and D2 (green) between the metal centres (M). These distances are crucial for understanding the cage's spatial arrangement and potential encapsulation capacity, particularly in relation to guest molecules such as cisplatin. The precise control of these distances can influence the structural stability and encapsulation efficiency of the metallacage.

6.3 The distances for Endo-N Cage

To analyze the Endo-N metallacages, we have measured two essential structural parameters: the distance between the metal centres on the top and bottom of the cage and between the carbon atoms at the equatorial centre (Figure 4). These measurements are crucial for evaluating the geometry and symmetry of the Endo-N cages. Understanding these parameters helps assess the cages' stability and potential effectiveness for applications such as cisplatin encapsulation. The geometric characteristics provide valuable insights into the structural integrity and functionality of the Endo-N cages in drug delivery systems.

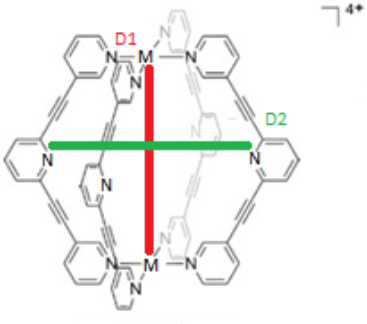

Figure 4: Distance between two metal ions (D1) and the N atoms on the side of the structure (D2)

The figure is a schematic diagram showing a top-down view of a metallacage structure. It emphasises the critical distances D1 (shown in red) and D2 (shown in green) between the metal centres (M). These distances are essential for comprehending the cage's spatial configuration and possible capacity to encapsulate guest molecules like cisplatin. Accurately manipulating these spacings can impact the structural stability and effectiveness of encapsulating substances within the metallacage.

3. Results and Discussion

Two distinct sections structure the investigation into cisplatin encapsulation within metallacages: the first section, Investigation of Empty Cages, evaluates the structural and stability characteristics of the metallacages in their unoccupied state, while the second section, Investigation of Encapsulation, assesses the effectiveness of the metallacages in encapsulating cisplatin and explores the implications for cisplatin delivery.

3.1 Investigation of Empty Cages

Two critical investigations have been undertaken to comprehensively understand the fundamental structure of metallacages: (i) Energy Minimisation and (ii) Geometry Optimisation.

Energy minimisation

Table 1 presents the minimised energies of various empty metallacages calculated using Hartree-Fock (HF) and PBE0 theories with the LanL2DZ basis set. The results reveal notable variations in energy differences between the HF and PBE0 methods across different metallacages. For instance, the Endo-N Pd2L4 cage exhibits an energy difference of 20.541 Hartree between HF and PBE0, while the Endo-N Au2L4 cage shows a difference of 20.635 Hartree. These discrepancies highlight that PBE0 generally predicts lower energy values compared to HF. This trend is consistent with the "Jacob's ladder" of exchange-correlation functionals, where PBE0, as a hybrid functional, incorporates both PBE and Hartree-Fock (HF) components, addressing some of the limitations inherent in pure DFT and HF methods. PBE0's lower energy predictions are attributed to its improved treatment of electron correlation and exchange interactions, leading to a more accurate depiction of the metallacages' stability and electronic structure. This higher level of accuracy shows that hybrid functionals are better than pure HF and PBE methods. So, the differences in energy that have been seen are significant for comparing and evaluating the theoretical frameworks used for these structures.

Table 1: Minimised Energies of Empty Metallacages Calculated Using Hartree Fock and PBE0 Theories with LanL2DZ Basis Set

Metallacages	Theories		Energy Difference
	Hartree Fock/LanL2DZ	PBE0/LanL2DZ	(EHF/LanL2DZ-EPBE0/LanL2DZ)
Endo-N Pd2L4	-3803.432	-3823.974	20.541
Endo-C Pd2L4	-3739.57	-3760.244	20.674
Endo-N Pt2L4	-3788.268	-3808.871	20.602
Endo-C Pt2L4	-3724.406	-3744.871	20.464
Endo-N Ni2L4	-3888.555	-3909.074	20.519
Endo-C Ni2L4	-3824.406	-3845.073	20.667
Endo-N Cu2L4	-3941.589	-3962.644	21.055
Endo-C Cu2L4	-3877.716	-3898.639	20.922
Endo-N Au2L4	-3822.055	-3842.691	20.635
Endo-C Au2L4	-3755.141	-3775.638	20.497

This table presents the minimised energies of various empty metallacages, each containing metal centres (Pd, Pt, Ni, Cu, Au) and ligands (Endo-N, Endo-C). We calculate the energies using two quantum chemical methods: Hartree Fock (HF) and PBE0, utilising the LanL2DZ basis set. We report the energy values in Hartree. The third column displays the energy differences between the Hartree Fock and PBE0 calculations, highlighting these two methods' discrepancies. When modelled with different theoretical approaches, these differences can provide insight into the cages' relative stability and electronic structure. We designate the metallacages as ML, where M stands for the metal ion,

and L is for the ligand. The data reveal trends in the energy differences influenced by choice of metal and the ligand environment.

The consistency of the lower energy values obtained from the PBE0 functional across these metal-based cages suggests a more accurate description of electronic interactions. Among the candidates, the Endo-C Cu2 L4 cage is the most promising, with the lowest energy value of -3962.644 Hartree. The second most promising candidate is the Endo-n Ni2L4 cage, with an energy of -3909.074 Hartree. In contrast, the Endo-C Pd2L4 cage is the least promising, with an energy of -3760.244 Hartree. Therefore, this study suggests that other empty cage structures may be more promising based on their energy minimisation results, even though wet lab techniques have published and validated the Pd2L4 cage.

The other result from Table 1 is that all Endo-N cages are more stable than the Endo-C cages because of lower energies. The lower energy means it is closer to the ground state energy. More H-bonds on the Endo-N cage may enhance the encapsulation process, and the crucial interaction between the host and guest can enhance the robustness of the complex, thereby facilitating drug delivery to the target. Consequently, Endo-n metallacages should be prioritised over and-C cages for cisplatin encapsulation.

Geometry Optimisation

Table 2 presents energy calculations for the geometry optimisation of various empty metallacages using Hartree-Fock (HF) and PBE0 theories with the LanL2DZ basis set. The energy differences between these methods are generally consistent across different metallacages, ranging from approximately 20.441 to 20.969 Hartree (Table 2). This difference shows that PBE0 always gives lower energy values than HF, which means that it gives a more accurate picture of how electrons interact in metallacage. Similar to the results from energy minimisation, PBE0 also proves superior to HF in geometry optimisation. Because PBE0 is a hybrid that combines Hartree-Fock exchange and PBE correlation, it can show more complex electron correlation effects. This gives a more accurate picture of the stability and electronic structure of metal lacquers. These insights are crucial for evaluating the potential performance of metallacages in applications such as cisplatin encapsulation, where accurate stability predictions are essential.

Table 2: Energy Calculations for Geometry Optimisation of Various Empty Metallacages Using Hartree Fock and PBE0 Theories with LanL2DZ Basis Set.

Metallacages	Theories		Energy Difference
	Hartree Fock/LanL2DZ	PBE0/LanL2DZ	(EHF/LanL2DZ-EPBE0/LanL2DZ)
Endo-N Pd_2L_4	-3803.776	-3824.291	20.515
Endo-C Pd_2L_4	-3739.892	-3760.272	20.379
Endo-N Pt_2L_4	-3788.606	-3809.185	20.579
Endo-C Pt_2L_4	-3724.725	-3745.166	20.441
Endo-N Ni_2L_4	-3888.555	-3909.358	20.803
Endo-C Ni_2L_4	-3824.670	-3845.338	20.668
Endo-N Cu_2L_4	-3941.817	Fail	Fail
Endo-C Cu_2L_4	-3877.925	-3898.895	20.969
Endo-N Au_2L_4	-3822.141	-3842.746	20.605
Endo-C Au_2L_4	-3755.415	-3775.938	20.524

This table presents the energies obtained from the geometry optimisation of different empty metallacages, each with distinct metal centres (Pd, Pt, Ni, Cu, Au) and ligands (Endo-N, Endo-C). The energies are calculated using two quantum chemical methods: Hartree-Fock (HF) and PBE0, both employing the LanL2DZ basis set. The energy values are reported in Hartree. The third column shows the energy difference between the Hartree-Fock and PBE0 calculations, which provides insights into the variation in energy predictions between these methods. This difference can reveal the relative stability of the optimised structures under different theoretical treatments. Notably, for the Endo-N Cu_2L_4 cage, the PBE0 optimisation failed, and consequently, the energy difference could not be calculated for this structure. The reason for failure is that the Endo-N Cu_2L_4 cage lacks energy convergence because of small energy fluctuations.

The energy calculations reveal that the Endo-N Ni2L4 and Endo-C Cu2L4 cages are the most promising candidates for cisplatin encapsulation based on their stability and energy estimates (Table 2). They provided the lowest energies with -3909.358 and -3898.895 Hartree, respectively. Although the Endo-C Cu2L4 cage was one of the most stable cages, the Endo-N Cu2L4 cage failed to find a stable structure once PBE0 was used in geometry optimisation. Also, Endo-C Pt2L4 showed the highest energy with -3745.166 Hartree, indicating that Endo-C Pt2L4 is the least stable metallacage. Consequently, geometry optimisation suggested novel metallacages for cisplatin encapsulation instead of the Pd2L4 cage.

Two distinct sections were examined to investigate the structural characteristics of empty metallacages: (i) Endo-C Cages Geometry Optimisation and (ii) Endo-N Cages Geometry Optimisation. These sections focus on optimising the geometry of cages with different metal centres to assess their stability and suitability for applications such as cisplatin encapsulation.

Endo-C Cages Geometry Optimization Analysis

To investigate the empty metallacages, Figure 5 provides visual representations of the structural configurations for four Endo-C M2L4 cages with different metal centres: Pt2L4, N2L4, Cu2L4, and Au2L4. These representations illustrate the cages' diverse geometries and coordination environments, clearly comparing their structural features.

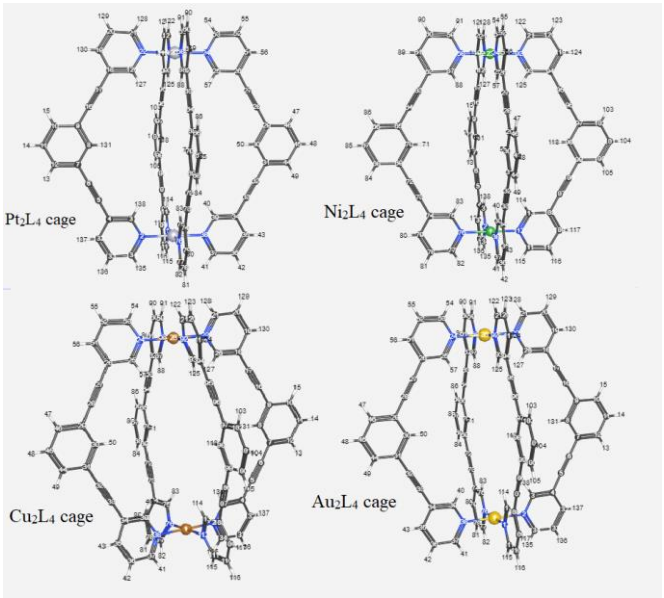

Figure 5: Structural representations of four Endo-C M2L4 cages with metal centres: Pt2L4, Ni2L4, Cu2L4, and Au2L4.

Each cage is shown with its respective metal centres (Pt, Ni, Cu, Au) coordinated by four ligands (L), forming highly symmetrical, elongated structures. These metallacages are investigated for their potential to encapsulate cisplatin molecules, with their geometry playing a critical role in determining the feasibility and efficiency of encapsulation.

Figure 5 visually represents empty Endo-C metallacages with different metal centres: Pt2L4, Ni2L4 , Cu2L4, and Au2L4. Among these, the Cu2L4 cage exhibits a distorted shape and loses its sharp symmetry, potentially hindering its ability to encapsulate cisplatin effectively, although the Endo-c Cu2L4 cage has provided the lowest energy in geometry optimisation among all Endo-c cages. In contrast, the Pt2L4, Ni2L4, and Au2L4 cages maintain a more defined geometry and symmetry, making them more viable

alternatives to the Pd2L4 cage. The enhanced structural stability of these three cages suggests their potential superiority in encapsulating cisplatin and improving the efficacy of drug delivery systems.

The internal volume of each metallacage was calculated by measuring the distances between metal centres on the top and bottom and the distances between carbon atoms at the equatorial centre. These volume calculations, presented in Table 3, are essential for understanding the structural characteristics of the metallacages. The size of the internal cavity significantly influences encapsulation efficiency; larger volumes can lead to weaker interactions between the cage (host) and the encapsulated cisplatin (guest), potentially causing premature drug release. Therefore, optimising cage volume is crucial to ensure that cisplatin remains securely encapsulated until it reaches its intended target, thereby enhancing the effectiveness of the drug delivery system.

Table 3: The distances, D1 and D2, and the approximate volume of the Endo-c cages.

Metallacages	in A (D1 in red)	A (D2 in green)	Volume A3	[Vx-VPd]	Radius in pm
Pd_2L_4	11.892	11.039	98.457	0% (as reference)	169
Pt_2L_4	11.814	11.027	97.705	-0.76%	177
Ni_2L_4	11.854	10.772	95.768	-2.73%	149
Cu_2L_4	11.843	11.000	97.705	-0.76%	145
Au_2L_4	11.973	11.025	99.002	0.55%	174

The table presents the vital geometrical parameters and volumes of various metallacages encapsulating cisplatin. The distances D1 (in red) and D2 (in green) represent the two primary diagonal distances within the cages, measured in Angstroms° (Å)°. The average volume of each cage is calculated in cubic Angstroms° (Å³), with the volume difference (Δvolume) indicating the percentage change compared to the reference Pd2L4 cage. Additionally, the atomic radii of the metals used in the cages are provided in picometres (pm) to illustrate their influence on the overall cage dimensions and volume.

The variation in metal atomic radii among the cages influences their internal volumes. For instance, the Pd2L4 cage has a metal atomic radius of 169 pm, while the Pt2L4 and Au2L4 cages have slightly larger radii (177 pm and 174 pm, respectively). The Ni2L4 and Cu2L4 cages have smaller radii (149 pm and 145 pm, respectively). This correlation suggests that larger metal atoms may contribute to a slightly increased cage volume, which could impact encapsulation efficiency. However, a larger volume does not necessarily guarantee better performance, as seen from the variations in percentage volume differences.

The volume calculations presented in Table 3 reveal that the Endo-c Au2L4 cage has the largest volume among the cages evaluated, at approximately 99.002 Å³. Also, the Endo-c Pd2L4 cage, as a validated metallacage for cisplatin encapsulation, has slightly smaller volumes, 98.456 Å³. Therefore, the Endo-c Au2 L4 cage can be an option to encapsulate more than one cisplatin molecule because of its higher volume than the Pd2L4 cage. The higher volume for Endo-c Au2 L4 can originate from the higher charge on Au than others with excessive +1 charge. However, its redox-active nature, transitioning between Au+3, Au+1, and Au, might introduce stability challenges for encapsulation. Also, the Cu2L4 cage, despite having a volume close to Pt2 L4, suffers from a distorted shape, impairing its encapsulation efficiency, mainly for two cisplatin molecules. The Pt2L4 cage, with its more stable geometry, presents a better alternative. On the other hand, the Endo-c Ni2L4 cage provided the smallest inside value with 95.768 Å³ (2.73% smaller compared to Pd2L4), which may not be large enough to contain more than one cisplatin for encapsulation.

Overall, while the Endo-C Pd2L4 cage remains the established choice for cisplatin encapsulation, the Endo-C Au2L4 cage offers a comparable alternative. The Endo-c Cu2L4 and Endo-c Pt2L4 cages present varying degrees of potential based on their volume and structural stability. The Endo-c Ni2L4 cage's reduced volume poses challenges to encapsulating one or two cisplatin molecules.

Endo-N Cages Geometry Optimization Analysis

To examine the empty metallacages, Figure 6 visually displays the structural configurations for four Endo-N M2L4 cages with varying metal centres: Pd2L4, Pt2L4, Ni2L4, and Cu2L4.

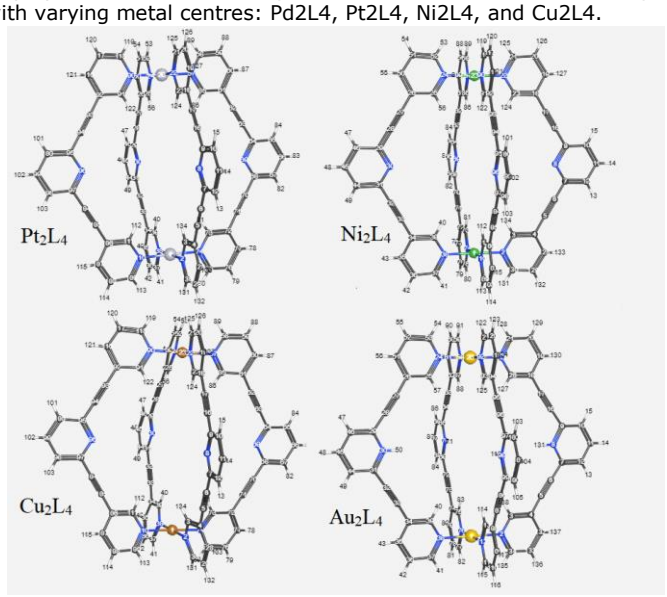

Figure 6: The structures of Endo-N empty M2L4 cages after geometry optimisation.

Each cage is shown with its respective metal centres (Pt, Ni, Cu, Au) coordinated by four ligands (L), forming highly symmetrical, elongated structures. These cages exhibit a high degree of symmetry and are characterised by elongated, cylindrical shapes, which are relevant for their potential application in encapsulating cisplatin molecules. Also, while geometry optimisation has not been completed for Endo-n Cu2L4 because of small energy fluctuation, its distorted shape has been shown in the figure.

Endo-n cages in Figure 6 demonstrated similar outputs with Endo-c cages in Figure 5. Shortly, Cu2L4 lost sharp symmetry, while the other provided promising structures.

Table 4: The distances, D1, and D2, and the approximate volume of the Endo-n cages

Metallacages	in A (D1 in red)	A (D2 in green)	Volume A3	[Vx-VPd]	Radius in pm
Pd_2L_4	11.532	11.196	96.834	0% (as reference)	169
Pt_2L_4	11.537	11.171	96.66	-0.18	177
Ni_2L_4	11.557	10.928	94.721	-2.182	149
Cu_2L_4	N/A	N/A	N/A	N/A	145
Au_2L_4	11.672	11.767	103.001	6.369	174

The table shows the diagonal distances D1 and D2 (in Angstroms) for various metallacages encapsulating cisplatin. The average volume is listed in cubic Angstroms (Å), with the percentage change in volume relative to the reference Pd2L4. The average volume of each cage is calculated in cubic Angstroms (Å³), with the volume difference (Δvolume) indicating the percentage change compared to the reference Pd2L4 cage. The atomic radii of the metals are measured in picometers (pm). Cu2L4 values are marked as N/A due to calculation issues.

Among the Endo-N cages, the Pt2L4 cage emerges as the most promising candidate for en-capsulation applications since its volume is close to that of the Pd2L4 cage, which has already demonstrated successful performance in cisplatin encapsulation (Table 4). The similarity in volume indicates that Pt2L4 could offer comparable conditions for effective drug encapsulation. On the

other hand, the Ni2L4 cage, with a 2.182% smaller volume than the Pd2L4 cage, while slightly smaller in volume, ranks as the second-best alternative for the Pd2L4 cage. However, the 2.182% reduced volume of the Ni2L4 cage might limit its effectiveness, particularly in accommodating the drug (Table 4). Also, the failure of Cu2L4 to complete the geometry optimisation for this cage indicates significant structural instability or distortion, which could severely impact its ability to encapsulate cisplatin. The results show that Cu2L4 is the least suitable option for encapsulation applications, as its compromised geometry will likely lead to inadequate binding and premature drug release. In addition, the Endo-N Au2L4 cage, which is 6.369% larger than the Pd2L4 cage, presents a unique case with its larger internal volume (Table 4). While this larger volume might suggest increased capacity, it also poses a risk of premature drug release due to weaker host-guest interactions.

The volumes of the Endo-N cages (Table 4) are generally smaller than their Endo-C counterparts (Table 3), except for the Au2L4 cage. The Endo-n Au2L4 cage stands out due to its significantly more extensive volume, increasing from 99.001 to 103.001 $Å^3$. Therefore, an Endo-N Au2L4 cage can be a rare opportunity to encapsulate two cisplatin molecules with the help of extensive volume. As for the other smaller Endo-N cages, they may not be promising for the encapsulation of two cisplatin molecules. Also, the lower volume may increase the molecular interaction between the cages and cisplatin, which may be a challenge for cisplatin release from the cages.

In terms of the total volume of the cages occupied by one cisplatin molecule, the results demonstrate a reduction compared to the empty cages. This reduction is attributed to the interactions between cisplatin and cage structure. The most significant change is observed in the Endo-C Cu2L4 cage, which is 2.02% larger than the occupied Pd2L4 cage. The proximity of cisplatin to the axis of the cage affects the angle between the metal centres and the drug, with variations observed across different cage types. For instance, the Endo-C Ni2L4, Pt2L4, and Au2L4 cages show slightly different angles than the Pd2L4 cage. These angular differences change the hydrogen bonding and van der Waals interactions, which in turn change how stable the drug-cage complex is. Weaker interactions and larger volumes could lead to premature drug release or reduced effectiveness.

The performance of the Cu2L4 cages, with their excess charge contributing to more robust interactions with cisplatin, contrasts with the lower performance of the Pt2L4 cages. The high charge on the Cu2L4 cages facilitates more robust binding, enhancing the stability of the encapsulated drug. Conversely, the lower stability of the Pt2L4 cages, evidenced by higher energy values, suggests that they are less effective in maintaining the encapsulated drug, potentially leading to faster drug release and reduced therapeutic efficacy.

In summary, the geometry optimisation results underscore the relative stability and effectiveness of the different cages in encapsulating cisplatin. The Cu2L4 cages, as demonstrated by their lowest energy values, show superior stability and interaction with cisplatin, making them the most promising candidates for drug delivery applications. Conversely, the Pt2L4 cages exhibit the highest energy levels, indicating lower stability and less favourable performance for drug encapsulation. The variations in cage volume and interaction angles further highlight the importance of precise structural optimisation in ensuring effective drug delivery. The strong binding observed with Cu2L4 cages and their lower energy states suggests their potential for enhanced drug retention and controlled release. These findings provide valuable insights into the design and selection of metallacages for optimised drug encapsulation and delivery systems.

6.4 Observation of cisplatin

Cisplatin undergoes energy minimisation and geometry optimisation to identify its most stable and realistic structure. Energy minimisation adjusts the molecule to reduce its total energy, ensuring it is in its lowest energy state. Geometry optimisation then refines the arrangement of atoms and bond angles to achieve the most stable configuration. This process is crucial for determining the hybridisation of palladium in cisplatin, which is d2sp3, resulting in a square planar geometry. These optimisations are essential for predicting the molecule's behaviour and interactions and critical for evaluating its performance in various applications.

Table 5: The energy minimisation and geometry optimisation (in Hartree) of cisplatin

Method	Hartree Fock/LanL2DZ	PBE0/LanL2dZ	Difference (EHartree-EPBE0)
Energy minimisation	-259.236	-261.237	2.001
Geometry optimisation	-259.236	-261.237	2.001

This table compares the results of energy minimisation and geometry optimisation for cisplatin using two different computational methods: Hartree-Fock with the LanL2DZ basis set and PBE0 with the LanL2DZ basis set. The final column shows the difference in energy between the two methods, highlighting how the choice of method affects the computed energy. Both energy minimisation and geometry optimisation yielded identical results in terms of energy difference, emphasising the consistency of the calculations across different methods.

The table presents the energy minimisation and geometry optimisation results for cisplatin using Hartree-Fock/LanL2DZ and PBE0/LanL2DZ methods. Both methods yield the same energy values for energy minimisation and geometry optimization. However, the PBE0 functional results in lower energy than Hartree-Fock, with a difference of 2.001 Hartree. The figures indicate that the PBE0 method provides a more stable and energetically favourable structure for cisplatin, highlighting its superior accuracy in modelling the molecule's potential energy surface.

3.2 The investigation of encapsulation of cisplatin via metallacages

Encapsulating two cisplatin molecules, as opposed to one, can significantly impact the effectiveness of the drug delivery system. The primary difference lies in the potential for increased therapeutic efficacy and controlled release. A single cisplatin molecule might not provide the desired therapeutic dose or stability, whereas encapsulating two molecules could enhance the overall efficacy by allowing for a higher drug load [98, 99, 100, 101]. Additionally, dual encapsulation might offer better control over the release kinetics, potentially leading to more effective targeting of cancer cells and reduced side effects [102, 103, 104]. Therefore, investigating the encapsulation of one versus two molecules is crucial for optimising the performance of metallacage-based drug delivery systems. Understanding how these cages perform with different drug loads makes it possible to design systems that maximise therapeutic outcomes while minimising premature drug release. Therefore, the investigation has been divided into (i) Single Cisplatin Molecule Encapsulation Analysis and (ii) Two Cisplatin Molecules Encapsulation Analysis.

Single Cisplatin Molecule Encapsulation Analysis

Single cisplatin molecule encapsulation analysis contains three subsections: (i) Energy Minimisation for Encapsulation of Single Cisplatin Molecule, (ii) Geometry Optimisation for Encapsulation of Single Cisplatin Molecule, and (iii) Visual representation of single cisplatin molecule encapsulation.

Energy Minimisation for Encapsulation of Single Cisplatin Molecule

The energy minimisation results presented in Table 6 provide valuable insights into the stability of various cage-cisplatin complexes. Notably, the Endo-N Cu2L4 complex achieved the lowest energy value of -4226.056 Hartree. However, it is essential to highlight that this complex failed to achieve energy convergence without cisplatin (as shown in Table 6). Table 6 indicates that cisplatin stabilises the Endo-N Cu2L4 metallacage, facilitating energy convergence. Similarly, the Endo-N Ni2L4 metallacage demonstrated the second-lowest energy, with a value of -4171.097 Hartree, suggesting it is also relatively stable. Regrettably, the Endo-C Pt L and Endo-C Pd2L4 complexes displayed higher energy levels of -4004.031 and -4019.187 Hartree, respectively, suggesting that these cages are less stable and deviate further from their ground-state energy. This trend aligns with earlier assessments, reinforcing that the Pt2L4 and Pd2 L4 cages may be less favourable for cisplatin encapsulation due to their higher energies and reduced stability. Overall, the lower energy values associated with Ni2L4 and Cu2L4 cages highlight their potential advantages over Pd2L4, Pt2L4 and Au2L4 cages. To enhance the effectiveness of cisplatin delivery systems, these stability challenges should be addressed in future research and validated through experimental studies.

Table 6: The energy minimisation of cage-cisplatin complex (one molecule of cisplatin)

Metallacages	Theories		Energy Difference
	Hartree Fock/LanL2DZ	PBE0/LanL2DZ	(EHF/LanL2DZ-EPBE0/LanL2DZ)
Endo-N Pd2L4	-4063.279	-4086.001	22.722
Endo-C Pd2L4	-3996.649	-4019.187	22.538
Endo-N Pt2L4	-4048.061	-4070.846	22.784
Endo-C Pt2L4	-3981.430	-4004.031	22.601
Endo-N Ni2L4	-4148.125	-4171.097	22.973
Endo-C Ni2L4	-4081.494	-4104.281	22.757
Endo-N Cu2L4	-4203.032	-4226.056	23.024
Endo-C Cu2L4	-4134.940	-4157.941	23.001
Endo-N Au2L4	-4080.511	-4103.318	22.807
Endo-C Au2L4	-4011.826	-4034.467	22.640

This table summarises the energy minimisation results for various cage-cisplatin complexes using two computational methods: Hartree-Fock with the LanL2DZ basis set and PBE0 with the LanL2DZ basis set. The final column presents the energy difference between these two methods, indicating the relative energy stabilisation that different cages contribute to the complex. The energy values highlight the subtle yet significant variations in stabilisation depending on the metal centre (Pd, Pt, Ni, Cu, Au) and the encapsulation mode (Endo-N or Endo-C).

Geometry Optimisation for Encapsulation of Single Cisplatin Molecule

Table 7 shows the outputs of the geometry optimisation. While the Hartree Fock method did not complete the optimisation for both Cu2L4 metallacages, the better PBE0/LanL2DZ method successfully provided results for metallacages. Consequently, this discrepancy highlights the enhanced accuracy of hybrid functionals like PBE0 over Hartree Fock, which is crucial for obtaining reliable energy assessments.

Table 7: The energy minimisation of cage-cisplatin complex (one molecule of cisplatin)

Metallacages	Theories		Energy Difference
	Hartree Fock/LanL2DZ	PBE0/LanL2DZ	(EHF/LanL2DZ-EPBE0/LanL2DZ)
Endo-N Pd2L4	-3998.542	-4087.538	88.996
Endo-C Pd2L4	-3998.542	-4020.777	22.202
Endo-N Pt2L4	-4049.912	-4072.430	22.518
Endo-C Pt2L4	-3983.366	-4005.668	22.302
Endo-N Ni2L4	-4149.855	-4172.596	22.741
Endo-C Ni2L4	-4083.312	-4105.833	22.521
Endo-N Cu2L4	Fail	-4226.180	-
Endo-C Cu2L4	Fail	-4159.404	-
Endo-N Au2L4	-4080.346	-4102.954	22.608
Endo-C Au2L4	-4013.803	-4036.188	22.384

This table presents the energy values obtained after geometry optimisation of various cage-cisplatin complexes using two computational methods: Hartree-Fock with the LanL2DZ basis set and PBE0 with the LanL2DZ basis set. The energy differences between these methods are highlighted to demonstrate how each cage structure, depending on the metal centre (Pd, Pt, Ni, Cu, Au) and encapsulation mode (Endo-N or Endo-C), affects the overall energy stability of the complex. The results also indicate instances where the calculations failed for specific structures.

The Endo-N Cu2L4 cages exhibit the lowest energy values with -4226.180 Hartree, indicating a high level of stability, followed by Endo-N Ni2L4, Endo-C Cu2L4, and Endo-N Ni2L4. Notably, the Endo-C Pt2L4 and Endo-C Pd2L4 cages show the highest energy levels with -4005.668 and -4020.776 Hartree, respectively. The higher energy suggests they are the least stable and, therefore, the least favourable for cisplatin encapsulation among the cages tested. Consequently, the lower energy values of Ni2L4 and Cu2L4 cages indicate potential advantages compared to Pd2L4, Pt2L4, and Au2L4 cages.

Visual representation of single cisplatin molecule encapsulation

Figure 7 illustrates the encapsulation of a single cisplatin molecule within the Endo-C and Endo-N Pd2L4 cages. Despite the differences in the coordination environments, both cages have effectively encapsulated cisplatin, as confirmed by experimental studies in wet labs. This successful encapsulation highlights the ability of these metallacages to securely contain and potentially deliver cisplatin, showcasing their practical applicability in drug delivery systems. The visual representation underscores (Figure 7) the compatibility of the cage structures with cisplatin and reinforces their potential as efficient carriers for targeted therapy.

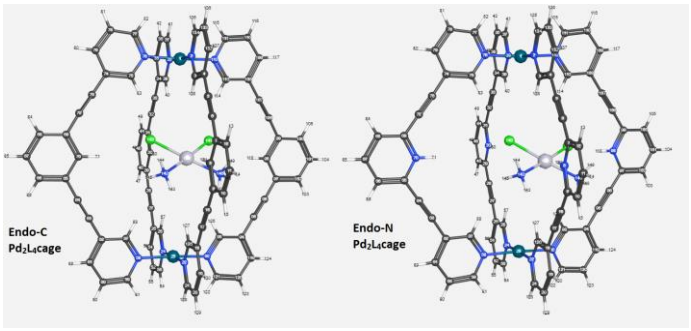

Figure 7: The structure of Endo-C and Endo-N Pd2L4 cages

The first metallacage represents Endo-C, and the second shows Endo-N. Both Endo-C and Endo-N metallacages contain one molecule of cisplatin.

The other Endo-C and Endo-N cages using Pt2+, Ni2+, Cu2+ and Au3+ have been visited in the figure to encapsulate cisplatin. Fortunately, all of them successfully encapsulate the cisplatin. All cages (Figure 8) can encapsulate one cisplatin molecule. The distortion of both Endo-N and Endo-C Cu2L4 cages can impact the drug's realisation, disrupt the drug-cage complex's distribution, and pose challenges in solution.

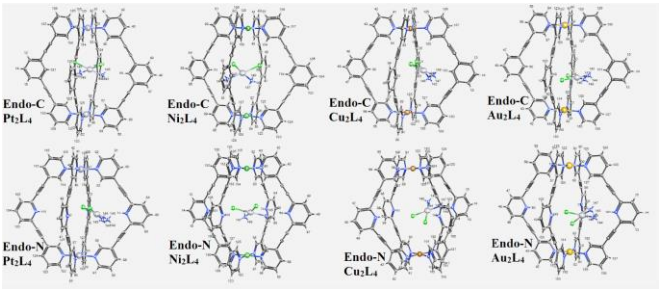

Figure 8: The structure of M2L4 cages occupied by cisplatin (one molecule).

The structures are divided into endohedral (Endo-C) and exohedral (Endo-N) configurations with varying metal centres: Pt2L4, Ni2L4, Cu2L4, and Au2L4. Each metal-ligand (M2L4) complex demonstrates distinct geometric arrangements and bonding interactions, which influence cisplatin's encapsulation efficiency and stability.

Figure 8 illustrates the encapsulation of cisplatin within various metallacages. While the cis-platin has been located in the centre of cages, including Endo-C Pt2L4, Endo-C Ni2L4, and Endo-N Ni2L4, cisplatin has been located in the edge of cages for the others. In particular, a cisplatin model has been furthest from the centre for both Au2L4 cages. Nevertheless, each cage has been successfully encapsulated with cisplatin for safe drug delivery without toxicity and drug resistance.

Two Cisplatin Molecules Encapsulation Analysis

Two molecules of cisplatin encapsulation analysis have been completed in three sections: (i) Energy Minimisation for Encapsulation of Two Cisplatin Molecules, (ii) Geometry Optimisation for Encapsulation of Two Cisplatin Molecules, and (iii) Visual representation of two cisplatin molecules encapsulation.

Energy Minimisation for Encapsulation of Two Cisplatin Molecules

Table 8 shows that the energy minimisation results indicate that the Endo-N Cu2L4 cage exhibits the lowest energy among the evaluated complexes, with a value of -4486.1817 Hartree using the PBE0/LanL2DZ method. This suggests that the Endo-N Cu2L4 cage is the most stable for encapsulating two cisplatin molecules. Following this, the Endo-N Ni2L4 cage has the second lowest energy of -4432.573 Hartree, and the Endo-C Cu2L4 cage ranks third with an energy of -4419.460 Hartree. Conversely, the least stable cages based on energy are the Endo-C Pt2L4 and Endo-C Pd2L4, with higher energy values of -4265.718 and -4280.832 Hartree, respectively. The general trend observed is that the "Endo" conformation combined with Cu2L4 and Ni2L4 tends to provide the lowest energy states, suggesting enhanced stability for these configurations compared to those involving Pt2L4 and Pd2L4.

Table 8: The energy minimisation of two molecules of cisplatin in the cages

Metallacages	Theories		Energy Difference
	Hartree Fock/LanL2DZ	PBE0/LanL2DZ	(EHF/LanL2DZ-EPBE0/LanL2DZ)
Endo-N Pd2L4	-4323.133	-4347.553	24.420
Endo-C Pd2L4	-4256.686	-4280.832	24.147
Endo-N Pt2L4	-4307.960	-4332.439	24.479
Endo-C Pt2L4	-4241.513	-4265.718	24.205
Endo-N Ni2L4	-4407.892	-4432.573	24.681
Endo-C Ni2L4	-4341.446	-4365.853	24.407
Endo-N Cu2L4	-4461.260	-4486.182	24.921
Endo-C Cu2L4	-4394.775	-4419.460	24.685
Endo-N Au2L4	-4338.196	-4362.779	24.583
Endo-C Au2L4	-4271.887	-4296.111	24.224

The table compares the total energy (in Hartree) of two cisplatin molecules within different cages, calculated using two different computational theories: Hartree-Fock with LanL2DZ basis set and PBE0 with LanL2DZ basis set. The last column shows the energy difference between the Hartree-Fock and PBE0 methods.

The energy minimisation of cages occupied by two cisplatin molecules indicates almost the same results as the previous interpretation of the cages (Table 8), which supports the idea. The best alternative cages are Pt2L4 and Au2L4 instead of Pd2L4.

Geometry Optimisation for Encapsulation of Two Cisplatin Molecules

Regarding optimisation failures, the Hartree-Fock method failed to optimise the geometry for several cages, including Endo-N Pd2L4, Endo-N Pt2L4, Endo-N Ni2L4, Endo-C Ni2L4, Endo-N Cu2L4, and Endo-C Cu2L4. Additionally, the PBE0 method failed for the Endo-C Ni2L4 and Endo-C Cu2L4 cages, indicating challenges in stabilising these configurations using these computational methods (Table 9).

Table 9: The geometry optimisation of two molecules of cisplatin in the cages

Metallacages	Theories		Energy Difference
	Hartree Fock/LanL2DZ	PBE0/LanL2DZ	(EHF/LanL2DZ-EPBE0/LanL2DZ)
Endo-N Pd2L4	Fail	-4347.749	-
Endo-C Pd2L4	-4256.904	-4278.774	21.871
Endo-N Pt2L4	Fail	-4332.634	-
Endo-C Pt2L4	-4241.724	-4265.917	-
Endo-N Ni2L4	Fail	-4432.801	-
Endo-C Ni2L4	Fail	Fail	-
Endo-N Cu2L4	Fail	-4486.396	-
Endo-C Cu2L4	Fail	Fail	-
Endo-N Au2L4	-4338.393	-4362.905	24.541
Endo-C Au2L4	-4271.909	-4296.181	24.272

After geometry optimisation for each cage, the table presents the final energies (in Hartree), calculated using Hartree-Fock with LanL2DZ basis set and PBE0 with LanL2DZ basis set. For cases where optimisation failed, the table indicates' Fail.' The energy difference between the Hartree-Fock and PBE0 methods is also provided, where applicable.

The geometry optimisation results highlight that the Endo-N Cu2L4 cage exhibits the lowest energy among the evaluated complexes, with a value of -4486.3963 Hartree using the PBE0/LanL2DZ method. The figures indicate that Endo-N Cu2L4 is the most stable configuration for encapsulating two cisplatin molecules. The second most stable complex is the Endo-N Ni2L4, with an energy of -4432.8015 Hartree, followed by the Endo-N Au2L4 cage at -4362.9054 Hartree. In contrast, the Endo-C Pt2L4 and Endo-C Pd2L4 cages are the least stable, with energies of -4265.9167 and -4278.7743 Hartree, respectively. The general trend indicates that cages with" Endo-N" configurations yield lower energies, suggesting higher stability than their "Endo-C" counterparts.

Visual representation of two cisplatin molecules encapsulation:

Figure 9 demonstrates the encapsulation of two cisplatin molecules within the Endo-C and Endo-N Pd2L4 cages. This dual encapsulation capability highlights the versatility and effectiveness of these metallacages in securing multiple drug molecules, which can enhance the overall therapeutic efficacy and control over drug release.

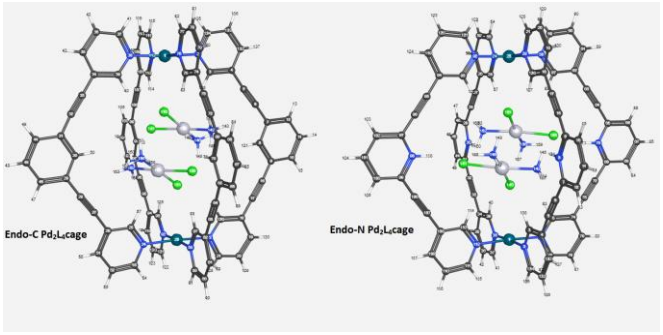

Figure 9: The structure of Endo-C and Endo-N Pd2L4 cages.

The initial metallacage indicates the Endo-C configuration, whereas the second one displays the Endo-N configuration. Both Endo-C and Endo-N metallacages each contain two molecules of cisplatin.

The other Endo-c and Endo-n cages using Pt2+, Ni2+, Cu2+, and Au3+ have been represented in Figure 9. Unfortunately, Endo-C Ni2+ and Endo-C Cu2+ have failed to encapsulate two cisplatin molecules. The other eight metallacages (Figures 9 and 10) successfully encapsulated two cisplatin molecules in the centre.

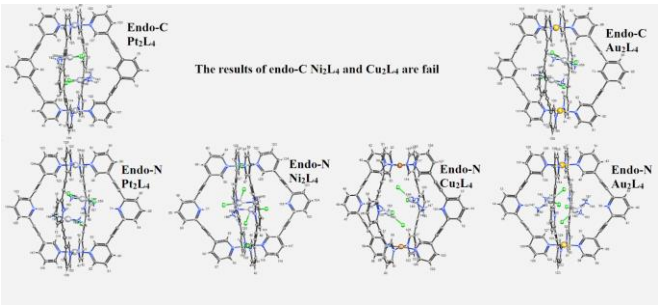

Figure 10: The structure of successful encapsulations of two cisplatin molecules inside the cages.

The structures are classified into endohedral (Endo-C) and exohedral (Endo-N). These configurations involve different metal centres, namely Pt2L4, Ni2L4, Cu2L4, and Au2L4. Every metal-ligand (M 2L4) complex exhibits unique geometric configurations and bonding interactions that impact cisplatin's encapsulation efficiency and stability.

Summary of Encapsulation Ability of Metallacages

The encapsulation abilities of various metallacages for cisplatin are summarised in Table 10. Every single metallacage showed the encapsulation of a single cisplaint. Also, except for Endo-C Ni2L4 and Endo-C Cu2L4, the other three metallacages could encapsulate the two molecules of cisplatin (Table 10).

Table 10: The overview of the encapsulation ability of the cages. (PPE0/LanL2DZ)

Metallacages	One molecule of cisplatin		Two molecules of cisplatin	
	Endo-C	Endo-N	Endo-C	Endo-N
Pd2L4	Yes	Yes	Yes	Yes
Pt2L4	Yes	Yes	Yes	Yes
Ni2L4	Yes	Yes	Fail	Yes
Cu2L4	Yes	Yes	Fail	Yes
Au2L4	Yes	Yes	Yes	Yes

The table shows whether each cage can encapsulate one or two molecules of cisplatin. The calculations are performed using the PBE0 functional and LanL2DZ basis set. The cages include metal centres: Pd, Pt, Ni, Cu, and Au. For each cage, the ability to encapsulate one or two molecules of cisplatin is indicated as" Yes" (successful encapsulation) or" Fail" (unsuccessful encapsulation).

Investigation of molecular interaction between host-guest

Several metallacages failed to complete the geometry optimisation process, marked as "Fail" in Table 11. Endo-N Cu2L4, Endo-C Ni2L4, Endo-C Cu2L4, and Endo-N Cu2L4 showed failures in both one and two cisplatin molecule encapsulations, suggesting that these structures might disassemble or become unstable during optimisation. These failures indicate that these metallacages are not suitable for stable encapsulation of cisplatin.

Single cisplatin molecule encapsulation

The best option for encapsulating a single cisplatin molecule is the Endo-N Ni2L4 metallacage, as it demonstrates the lowest energy at −4172.596 Hartree. The second-best option is Endo-N Pd2L4, with a slightly higher energy of −4087.538 Hartree. Conversely, the worst option among the successful cases is Endo-C Pt2L4, which exhibits a significantly higher energy of −4005.668 Hartree. These energy differences indicate the relative stability and effectiveness of each metallacage in encapsulating one cisplatin molecule.

The energy difference for one cisplatin molecule encapsulation provides further insight into the effectiveness of the metallacages. The Endo-N Ni2L4 cage shows the most negative energy difference of −2.001 Hartree, indicating a strong encapsulation interaction. On the other hand, Endo-C Pt2L4 shows a positive energy difference of 0.735 Hartree, suggesting weaker encapsulation. These differences underscore the superior performance of the Endo-N Ni2L4 cage in single cisplatin molecule encapsulation.

Two cisplatin molecules encapsulation

Regarding encapsulating two cisplatin molecules, Endo-N Ni2L4 again proves to be the best option, showing the lowest energy of −4432.801 Hartree. The second best is Endo-N Pd2L4, with an energy of −4347.748 Hartree. In contrast, Endo-C Pt2L4 is the worst option among the successful cases, with a significantly higher energy of −4265.917 Hartree. These energy values suggest that Endo-N Ni2L4 is the most stable and effective for encapsulating two cisplatin molecules.

The energy difference for encapsulating two cisplatin molecules reveals a similar trend. Endo-N Ni2L4 exhibits the most negative energy difference of −0.970 Hartree, indicating effective and stable encapsulation. In contrast, Endo-C Pt2L4 shows a less negative energy difference of 1.723 Hartree, reflecting a weaker encapsulation interaction. This comparison highlights the superiority of Endo-N Ni2L4 in encapsulating two cisplatin molecules.

Table 11: The overview of the encapsulation ability of the cages. (PPE0/LanL2DZ)

Metallacage	PBE0/LanL2DZ					
	The energy of geometry Optimisation in Hartree					
	Empty	Cisplatin	One molecule	Two molecules	Energy Difference in Hartree for one	Energy Difference in Hartree for two
Endo-N Pd2L4	-3824.291	-261.237	-4087.538	-4347.749	-2.010	-0.984
Endo-C Pd2L4	-3760.272	-261.237	-4020.777	-4278.774	0.732	3.971
Endo-N Pt2L4	-3809.185	-261.237	-4072.430	-4332.634	-2.008	-0.975
Endo-C Pt2L4	-3745.166	-261.237	-4005.668	-4265.917	0.735	1.723
Endo-N Ni2L4	-3909.358	-261.237	-4172.596	-4432.801	-2.001	-0.970
Endo-C Ni2L4	-3845.338	-261.237	-4105.833	Fail	0.742	Fail
Endo-N Cu2L4	Fail	-261.237	-4226.180	-4486.396	Fail	Fail
Endo-C Cu2L4	-3898.895	-261.237	-4159.404	Fail	0.727	Fail
Endo-N Au2L4	-3842.746	-261.237	-4102.954	-4362.905	1.029	2.314
Endo-C Au2L4	-3775.938	-261.237	-4036.188	-4296.181	0.987	2.231

The table displays the total energy of the metallacage in its empty state, the energy of cisplatin, and the energy of the encapsulated system for different metallacages, including Endo-N Pd_2L_4, Endo-C Pd_2L_4, Endo-N Pt_2L_4, Endo-C Pt_2L_4, Endo-N Ni_2L_4, Endo-C Ni_2L_4, Endo-N Cu $_2L_4$, Endo-C Cu_2L_4, Endo-N Au_2L_4, and Endo-C Au_2L_4. The energies are presented in Hartree units. Additionally, the distances (in Angstroms) between the encapsulated cisplatin and the metallacage for both one and two configurations are provided, highlighting variations in encapsulation strength and spatial arrangement. Some entries are marked as" Fail", indicating the structure has been disassembled a part, so the geometry optimisation has not been completed for the metallacage. This table facilitates comparisons of energy changes due to encapsulation across different metallacages and provides insights into the efficiency and stability of the encapsulated systems.

4. Future directions

4.1 Enhancing Computational Methods for Basis Set Optimization

Future work in metallacage research could focus on optimising the basis sets used in DFT calculations to improve the accuracy of predictions related to cisplatin encapsulation. While combining different basis sets like LanL2TZ and STO-2 has proven challenging due to limitations in WebMo and Gaussian 9, new approaches could involve the development of hybrid basis sets tailored specifically for metallacages. These hybrid sets would balance computational cost with accuracy, making it easier to simulate complex systems. Advanced GEN codes, which allow customisation of basis sets, could be explored further to achieve this balance. This would enable more precise energy calculations and geometry optimisations, leading to better predictions for metallacage behaviour.

4.2 Exploring New Exchange-Correlation Functionals

Another avenue for future research involves exploring novel exchange-correlation functionals, such as those found in Jacob's Ladder, to improve the accuracy of DFT calculations. While PBE0 and Hartree-Fock functionals have been commonly used, developing new functionals like Rung 3.5, which sits between semi-local and non-local, could offer better accuracy for modelling metallacages. These functionals might also help identify more suitable drug delivery candidates by better understanding the energy landscape and molecular interactions within these structures.

4.3 Expanding Metallacage Investigations

Research could also include a broader range of metallacages and related structures. Investigations into cages like Fe4L68+, Ag2L42+, and Hg2L44+ , as well as metallo-macrocycles, could yield valuable insights. Additionally, the potential of other transition metals, such as Ruthenium (Ru), Osmium (Os), Iridium (Ir), Rhodium (Rh), and Manganese (Mn), in forming stable and effective metallacages for drug delivery should be explored. These metals have shown promising characteristics similar to palladium, and their inclusion in DFT studies could lead to the discovery of new, efficient encapsulation systems.

4.4 Integrating Machine Learning for Efficient Analysis

The Density Functional Theory (DFT) approach has proven to be a powerful tool for understanding the encapsulation mechanisms and stability of metallacage-cisplatin complexes. However, its computational intensity presents significant challenges, particularly when scaling to larger systems or exploring a broader array of metallacage designs. As an alternative, machine learning (ML)-based models offer a promising avenue for addressing these challenges. ML models can rapidly predict critical properties such as binding energies, structural stability, and encapsulation efficiency by leveraging data-driven algorithms trained on existing DFT results. This approach has the potential to significantly reduce computational costs while maintaining a high degree of accuracy. Future research should focus on developing and validating such models, integrating them with experimental data to enhance their predictive capabilities, and expanding their application to diverse metallacage-drug systems [95, 96]. This synergistic use of DFT and ML could revolutionise the design and optimisation of cisplatin delivery systems, paving the way for more efficient and effective therapeutic solutions.

4.5 Broader Applications and Comparison with Other Systems

This study provides significant insights into the potential of metallacage-based systems for cisplatin encapsulation, but certain limitations should be acknowledged. First, while the computational approaches employed—PBE0 and Hartree Fock theories with the LanL2DZ basis set—are robust and suitable for studying metallacage stability, they may not fully capture all aspects of dynamic behavior or environmental interactions. Other computational methods, such as molecular dynamics simulations or hybrid quantum mechanics/molecular mechanics (QM/MM) approaches, could complement our findings by providing a more detailed picture of the interactions under physiological conditions. Additionally, the accuracy of the current results could be further validated by comparing with experimental data or exploring alternative computational techniques, such as more advanced dispersion-corrected density functional theory (DFT-D) methods.

The study study focused solely on the encapsulation of cisplatin. While cisplatin remains a cornerstone of chemotherapy, future work should explore the encapsulation of other clinically relevant drugs, such as carboplatin or oxaliplatin, to assess the generalizability of metallacage systems. Furthermore, different types of drug delivery mechanisms, including sustained release and targeted delivery systems, could be investigated to enhance the therapeutic potential of metallacages. This would require combining computational findings with experimental studies to evaluate their real-world efficacy and biocompatibility.

In addition to metallacages, cisplatin has been successfully encapsulated in various other supramolecular systems, such as liposomes, polymeric nanoparticles, and micelles. Liposomes, for instance, have been widely studied as drug delivery vehicles due to their biocompatibility and ability to encapsulate both hydrophilic and hydrophobic drugs. Similarly, polymeric nanoparticles can be engineered to deliver cisplatin in a controlled and sustained manner, minimizing side effects while enhancing therapeutic efficacy. However, comparing the performance of metallacages with these systems presents several challenges. Liposomes and polymeric nanoparticles typically rely on different encapsulation mechanisms, such as passive encapsulation or active targeting, which may differ significantly from the encapsulation process in metallacages. Moreover, these systems often involve complex synthesis procedures and may require modifications to optimize drug release profiles or improve stability under physiological conditions. While a direct comparison could offer valuable insights, such studies must account for these fundamental differences, including the drug release kinetics, stability, and bioavailability of each system. Thus, while alternative encapsulation systems like liposomes offer promising routes for cisplatin delivery, the unique characteristics of metallacages—such as their structural tunability and the potential for metal-ligand coordination—present distinct advantages and should be evaluated in their own right.

Lastly, while this work has demonstrated the superiority of Endo-N cages over Endo-C cages for cisplatin encapsulation, the broader applicability of these findings remains unclear. Future studies could explore alternative ligand designs and metal ions to expand the scope of metallacage systems. A systematic comparison of metallacages with other supramolecular delivery systems, such as metal-organic frameworks (MOFs) and micelles, would provide valuable insights into their relative advantages and limitations.

6. Conclusion

This research comprehensively analyses the encapsulation capabilities of various metallacages for cisplatin, evaluating their stability and effectiveness using the PBE0/LanL2DZ functional and basis set. Our findings indicate that the Endo-N Ni2L4 and Endo-N Cu2L4 metallacages emerge as the most effective candidates for both single and dual cisplatin molecule encapsulation. This metallacage demonstrated the lowest energy configurations for one and two cisplatin molecules and exhibited the most negative energy differences, highlighting its superior encapsulation performance.

In comparison, the Endo-C Pd2L4 metallacage, while successful in encapsulating cisplatin, did not match the stability and effectiveness of the Endo-N Ni2L4 cage. The Endo-C Pd2L4 showed higher energy values and less favourable energy differences, suggesting it is less optimal for encapsulating cisplatin compared to Endo-N Ni2L4. Additionally, several metallacages, including Endo-N Cu2L4 and Endo-C Cu2L4, failed to complete the geometry optimisation, indicating potential instability and unsuitability for effective cisplatin encapsulation.

Overall, this study underscores the importance of selecting the right metallacage for drug encapsulation applications. The Endo-N Ni2L4 metallacage is a superior choice due to its demonstrated stability and effectiveness in encapsulating single and dual cisplatin molecules. These results pave the way for further research into optimising metallacage-based encapsulation systems, potentially enhancing the design of advanced drug delivery mechanisms.

6. References

1. James C Dabrowiak. Metals in medicine. *Inorganica Chimica Acta*, 393:1–2, 2012.
2. Barnett Rosenberg, Loretta Vancamp, James E Trosko, and Virginia H Mansour. Platinum compounds: a new class of potent antitumour agents. *nature*, 222(5191):385–386, 1969.
3. Timothy C Johnstone, Kogularamanan Suntharalingam, and Stephen J Lippard. The next generation of platinum drugs: targeted pt (ii) agents, nanoparticle delivery, and pt (iv) pro-drugs. *Chemical reviews*, 116(5):3436–3486, 2016.
4. Dong Wang and Stephen J Lippard. Cellular processing of platinum anti-cancer drugs. *Nature reviews Drug discovery*, 4(4):307–320, 2005.
5. Zahid H Siddik. Cisplatin: mode of cytotoxic action and molecular basis of resistance. *Onco-gene*, 22(47):7265–7279, 2003.
6. Sumit Ghosh. Cisplatin: The first metal based anti-cancer drug. *Bioorganic chemistry*, 88:102925, 2019.
7. Takatoshi Karasawa and Peter S Steyger. An integrated view of cisplatin-induced nephrotox-icity and ototoxicity. *Toxicology letters*, 237(3):219–227, 2015.
8. GP Stathopoulos and T Boulikas. Lipoplatin formulation review article. *Journal of drug delivery*, 2012(1):581363, 2012.
9. Hardeep S Oberoi, Natalia V Nukolova, Alexander V Kabanov, and Tatiana K Bronich. Nanocarriers for delivery of platinum anti-cancer drugs. *Advanced drug delivery reviews*, 65(13-14):1667–1685, 2013.
10. Ana-Maria Florea and Dietrich B¨usselberg. Cisplatin as an anti-tumor drug: cellular mecha-nisms of activity, drug resistance and induced side effects. *Cancers*, 3(1):1351–1371, 2011.
11. Michail Nikolaou, Athanasia Pavlopoulou, Alexandros G Georgakilas, and Efthymios Kyrodi-mos. The challenge of drug resistance in cancer treatment: a current overview. *Clinical & Experimental Metastasis*, 35:309–318, 2018.
12. Xuan Wang, Haiyun Zhang, and Xiaozhuo Chen. Drug resistance and combating drug resis-tance in cancer. *Cancer drug resistance*, 2(2):141, 2019.
13. Andrea Schmidt. *Supramolecular metallocages as potential delivery systems for anti-cancer drugs*. PhD thesis, Technische Universit¨at M¨unchen, 2016.
14. Matthew D Hall, Mitsunori Okabe, Ding-Wu Shen, Xing-Jie Liang, and Michael M Gottesman. The role of cellular accumulation in determining sensitivity to platinum-based chemotherapy. *Annu. Rev. Pharmacol. Toxicol.*, 48(1):495–535, 2008.
15. Guocan Yu, Timothy R Cook, Yang Li, Xuzhou Yan, Dan Wu, Li Shao, Jie Shen, Guping Tang, Feihe Huang, Xiaoyuan Chen, et al. Tetraphenylethene-based highly emissive metal-lacage as a component of theranostic supramolecular nanoparticles. *Proceedings of the National Academy of Sciences*, 113(48):13720–13725, 2016.
16. Pieter CA Bruijnincx and Peter J Sadler. New trends for metal complexes with anti-cancer activity. *Current opinion in chemical biology*, 12(2):197–206, 2008.
17. Timothy R Cook and Peter J Stang. Recent developments in the preparation and chemistry of metallacycles and metallacages via coordination. *Chemical reviews*, 115(15):7001–7045, 2015.
18. Alexander P¨othig and Angela Casini. Recent developments of supramolecular metal-based structures for applications in cancer therapy and imaging. *Theranostics*, 9(11):3150, 2019.
19. Guocan Yu, Meijuan Jiang, Feihe Huang, and Xiaoyuan Chen. Supramolecular coordination complexes as diagnostic and therapeutic agents. *Current opinion in chemical biology*, 61:19–31, 2021.
20. Feng Chen, Yang Li, Xiongjie Lin, Huayu Qiu, and Shouchun Yin. Polymeric systems con-taining supramolecular coordination complexes for drug delivery. *Polymers*, 13(3):370, 2021.
21. Angela Casini, Benjamin Woods, and Margot Wenzel. The promise of self-assembled 3d supramolecular coordination complexes for biomedical applications, 2017.
22. Yang Bai, Chunli Liu, Yuying Shan, Tingting Chen, Yan Zhao, Chao Yu, and Huan Pang. Metal-organic frameworks nanocomposites with different dimensionalities for energy conver-sion and storage. *Advanced Energy Materials*, 12(4):2100346, 2022.
23. Changfeng Yin, Jiaxing Du, Bogdan Olenyuk, Peter J Stang, and Yan Sun. The applications of metallacycles and metallacages. *Inorganics*, 11(2):54, 2023.
24. Yiliang Wang, Taotao Liu, Yang-Yang Zhang, Bin Li, Liting Tan, Chunju Li, Xing-Can Shen, and Jun Li. Cross-catenation between position-isomeric metallacages. *Nature Communica-tions*, 15(1):1363, 2024.
25. Yang Li, Jinjin Zhang, Hui Li, Yiqi Fan, Tian He, Huayu Qiu, and Shouchun Yin. Metallacycle/metallacage-cored fluorescent supramolecular assemblies with aggregation-induced emission properties. *Advanced Optical Materials*, 8(14):1902190, 2020.
26. Hajar Sepehrpour, Wenxin Fu, Yan Sun, and Peter J Stang. Biomedically relevant self-assembled metallacycles and metallacages. *Journal of the American Chemical Society*, 141(36):14005–14020, 2019.
27. Yida Pang, Chonglu Li, Hongping Deng, and Yao Sun. Recent advances in luminescent metallacycles/metallacages for biomedical imaging and cancer therapy. *Dalton Transactions*, 51(43):16428–16438, 2022.
28. Jens Bunzen, Junji Iwasa, Pia Bonakdarzadeh, Eri Numata, Kari Rissanen, Sota Sato, and Makoto Fujita. Self-assembly of m 24 l 48 polyhedra based on empirical prediction. *Angewandte Chemie International Edition*, 13(51):3161–3163, 2012.
29. Casey Sandra Christie. *New homoleptic and heteroleptic [Pd2L4] helicates.* PhD thesis, Uni-versity of Otago, 2021.
30. Puhong Liao, Brian W Langloss, Amber M Johnson, Eric R Knudsen, Fook S Tham, Ryan R Julian, and Richard J Hooley. Two-component control of guest binding in a self-assembled cage molecule. *Chemical communications*, 46(27):4932–4934, 2010.
31. Andrea Schmidt, Viviana Molano, Manuela Hollering, Alexander P¨othig, Angela Casini, and Fritz E K¨uhn. Evaluation of new palladium cages as potential delivery systems for the anti-cancer drug cisplatin. *Chemistry–A European Journal*, 22(7):2253–2256, 2016.
32. J Han, A Schmidt, T Zhang, H Permentier, GMM Groothuis, R Bischoff, FE K¨uhn, P Horvatovich, and A Casini. Bioconjugation strategies to couple supramolecular exo-functionalized palladium cages to peptides for biomedical applications. *Chemical Commu-nications*, 53(8):1405–1408, 2017.
33. William F Polik and JR Schmidt. Webmo: Web-based computational chemistry calculations in education and research. *Wiley Interdisciplinary Reviews: Computational Molecular Science*, 12(1):e1554, 2022.
34. Jorge Kohanoff. *Electronic structure calculations for solids and molecules: theory and compu-tational methods*. Cambridge university press, 2006.
35. Jake Graser, Steven K Kauwe, and Taylor D Sparks. Machine learning and energy minimiza-tion approaches for crystal structure predictions: a review and new horizons. *Chemistry of Materials*, 30(11):3601–3612, 2018.

36. CRA Catlow, ZX Guo, M Miskufova, SA Shevlin, AGH Smith, AA Sokol, Aron Walsh, DJ Wil-son, and SM Woodley. Advances in computational studies of energy materials. *Philosoph-ical Transactions of the Royal Society A: Mathematical, Physical and Engineering Sciences*, 368(1923):3379–3456, 2010.
37. Jun-Ichi Iwata, Daisuke Takahashi, Atsushi Oshiyama, Taisuke Boku, Kenji Shiraishi, Susumu Okada, and Kazuhiro Yabana. A massively-parallel electronic-structure calculations based on real-space density functional theory. *Journal of Computational Physics*, 229(6):2339–2363, 2010.
38. J Ulises Reveles and Andreas M K¨oster. Geometry optimisation in density functional methods. *Journal of computational chemistry*, 25(9):1109–1116, 2004.
39. Zoe L Seeger and Ekaterina I Izgorodina. etry optimisations of ionic liquid clusters. 16(10):6735–6753, 2020. A systematic study of dft performance for geom-*Journal of Chemical Theory and Computation*,
40. Xiaobin Liao, Ruihu Lu, Lixue Xia, Qian Liu, Huan Wang, Kristin Zhao, Zhaoyang Wang, and Yan Zhao. Density functional theory for electrocatalysis. *Energy & Environmental Materials*, 5(1):157–185, 2022.
41. Udo Schnupf and Frank A Momany. Dft energy optimisation of a large carbohydrate: cyclo-maltohexaicosaose (ca-26). *The Journal of Physical Chemistry B*, 116(23):6618–6627, 2012.
42. Robert Palmer, Steve Barrus, Yu Yang, Ganesh Gopalakrishnan, and Robert M Kirby. Gauss: A framework for verifying scientific computing software. *Electronic Notes in Theoretical Com-puter Science*, 144(3):95–106, 2006.
43. Ian D Chivers and Jane Sleightholme. *Introduction to programming with Fortran*, volume 2. Springer, 2018.
44. John A Trangenstein. *Scientific Computing*. Springer, 2017.
45. Trygve Helgaker, POUL JØRGENSEN, Jeppe Olsen, and Wim Klopper. Wave function based quantum chemistry. *Computational Medicinal Chemistry for Drug Discovery. New York–Basel: Marcel Dekker*, pages 57–87, 2004.
46. Peter MW Gill and Paul von Rague Schleyer. Density functional theory (dft), hartree-fock (hf), and the self-consistent field. *J. Chem. Phys*, 100:5066–5075, 1994.
47. M Ya Amusia, AZ Msezane, and VR Shaginyan. Density functional theory versus the hartree– fock method: Comparative assessment. *Physica Scripta*, 68(6):C133, 2003.
48. Matthias Ernzerhof and Gustavo E Scuseria. Assessment of the perdew–burke–ernzerhof exchange-correlation functional. *The Journal of chemical physics*, 110(11):5029–5036, 1999.
49. Joachim Paier, Robin Hirschl, Martijn Marsman, and Georg Kresse. The perdew–burke– ernzerhof exchange-correlation functional applied to the g2-1 test set using a plane-wave basis set. *The Journal of chemical physics*, 122(23), 2005.
50. Oleg A Vydrov and Gustavo E Scuseria. Assessment of a long-range corrected hybrid func-tional. *The Journal of chemical physics*, 125(23), 2006.
51. T Gavin Williams and Angela K Wilson. Importance of the quality of metal and ligand basis sets in transition metal species. *The Journal of chemical physics*, 129(5), 2008.
52. S Chiodo, Nino Russo, and Emilia Sicilia. Lanl2dz basis sets recontracted in the framework of density functional theory. *The Journal of chemical physics*, 125(10), 2006.
53. Victor Christianto. A review of schr¨odinger equation and classical wave equation. *Prespacetime Journal*, 5(5), 2014.
54. Robert Withnall, Babur Z Chowdhry, Stephen Bell, and Trevor J Dines. Computational chem-istry using modern electronic structure methods. *Journal of chemical education*, 84(8):1364, 2007.
55. Steven M Bachrach. *Computational organic chemistry*. John Wiley & Sons, 2014.
56. Christopher M Baker and Guy H Grant. Modeling aromatic liquids: toluene, phenol, and pyridine. *Journal of Chemical Theory and Computation*, 3(2):530–548, 2007.
57. Christopher J Cramer. *Essentials of computational chemistry: theories and models*. John Wiley & Sons, 2013.
58. Michael E Foster and Karl Sohlberg. Empirically corrected dft and semi-empirical methods for non-bonding interactions. *Physical chemistry chemical physics*, 12(2):307–322, 2010.
59. Georg Schreckenbach, P Jeffrey Hay, and Richard L Martin. Density functional calculations on actinide compounds: Survey of recent progress and application to [uo2x4] 2-(x= f, cl, oh) and anf6 (an= u, np, pu). *Journal of computational chemistry*, 20(1):70–90, 1999.
60. David A Dixon, Thom H Dunning, Michel Dupuis, David Feller, Deborah Gracio, Robert J Harrison, Donald R Jones, Ricky A Kendall, Jefferey A Nichols, Karen Schuchardt, et al. Com-putational chemistry in the environmental molecular sciences laboratory. In *High-Performance Computing*, pages 215–228. Springer, 1999.
61. Trygve Helgaker, Sonia Coriani, Poul Jørgensen, Kasper Kristensen, Jeppe Olsen, and Ken-neth Ruud. Recent advances in wave function-based methods of molecular-property calcula-tions. *Chemical reviews*, 112(1):543–631, 2012.
62. Jonathan Thirman and Martin Head-Gordon. tron correlation in intermolecular interactions. 5(8):1380–1385, 2014. Electrostatic domination of the effect of elec-*The Journal of Physical Chemistry Letters*,
63. Biswajit Santra. *Density-functional theory exchange-correlation functionals for hydrogen bonds in water*. PhD thesis, Technische Universit¨at Berlin Berlin, 2010.
64. Mar´ıa Luisa Senent and S Wilson. Intramolecular basis set superposition errors. *International journal of quantum chemistry*, 82(6):282–292, 2001.
65. Yue Yang, Michael N Weaver, and Kenneth M Merz Jr. Assessment of the "6-31+ g**+ lanl2dz" mixed basis set coupled with density functional theory methods and the effective core potential: prediction of heats of formation and ionisation potentials for first-row-transition-metal complexes. *The Journal of Physical Chemistry A*, 113(36):9843–9851, 2009.
66. Xin Xu and William A Goddard III. The extended perdew-burke-ernzerhof functional with improved accuracy for thermodynamic and electronic properties of molecular systems. *The Journal of chemical physics*, 121(9):4068–4082, 2004.
67. Reinhart Ahlrichs, Filipp Furche, and Stefan Grimme. Comment on "assessment of exchange correlation functionals"[aj cohen, nc handy, chem. phys. lett. 316 (2000) 160–166]. *Chemical Physics Letters*, 325(1-3):317–321, 2000.
68. Markus Bursch, Jan-Michael Mewes, Andreas Hansen, and Stefan Grimme. Best-practice dft protocols for basic molecular computational chemistry. *Angewandte Chemie International Edition*, 61(42):e202205735, 2022.
69. Friedhelm Bechstedt. Non-local exchange and correlation. In *Many-Body Approach to Elec-tronic Excitations: Concepts and Applications*, pages 163–195. Springer, 2014.
70. Jochen Heyd, Gustavo E Scuseria, and Matthias Ernzerhof. Hybrid functionals based on a screened coulomb potential. *The Journal of chemical physics*, 118(18):8207–8215, 2003.
71. Jochen Heyd, Juan E Peralta, Gustavo E Scuseria, and Richard L Martin. Energy band gaps and lattice parameters evaluated with the heyd-scuseria-ernzerhof screened hybrid functional. *The Journal of chemical physics*, 123(17), 2005.

72. Emmanuel Mitry, Pascal Hammel, Ga¨el Deplanque, Fran¸coise Mornex, Philippe Levy, Jean-Fran¸cois Seitz, Alain Moussy, Jean-Pierre Kinet, Olivier Hermine, Philippe Rougier, et al. Safety and activity of masitinib in combination with gemcitabine in patients with advanced pancreatic cancer. *Cancer chemotherapy and pharmacology*, 66:395–403, 2010.
73. Carl H Schiesser, Michelle L Styles, and Lisa M Wild. Ab initio study of some free-radical homolytic substitution reactions at silicon, germanium and tin. *Journal of the Chemical Society, Perkin Transactions 2*, (11):2257–2262, 1996.
74. Xuefei Xu and Donald G Truhlar. Accuracy of effective core potentials and basis sets for density functional calculations, including relativistic effects, as illustrated by calculations on arsenic compounds. *Journal of chemical theory and computation*, 7(9):2766–2779, 2011.
75. Tom´aˇs Kubaˇr and Marcus Elstner. A hybrid approach to simulation of electron transfer in complex molecular systems. *Journal of The Royal Society Interface*, 10(87):20130415, 2013.
76. Richard A Friesner. Ab initio quantum chemistry: Methodology and applications. *Proceedings of the National Academy of Sciences*, 102(19):6648–6653, 2005.
77. Igor Lyskov, Martin Kleinschmidt, and Christel M Marian. Redesign of the dft/mrci hamil-tonian. *The Journal of chemical physics*, 144(3), 2016.
78. Jos´e Canosa and Roberto Gomes De Oliveira. A new method for the solution of the schr¨odinger equation. *Journal of computational physics*, 5(2):188–207, 1970.
79. Brett Barwick, Glen Gronniger, Lu Yuan, Sy-Hwang Liou, and Herman Batelaan. A measure-ment of electron-wall interactions using transmission diffraction from nanofabricated gratings. *Journal of Applied Physics*, 100(7), 2006.
80. Roger Bach, Damian Pope, Sy-Hwang Liou, and Herman Batelaan. Controlled double-slit electron diffraction. *New Journal of Physics*, 15(3):033018, 2013.
81. Nika N Danial and Stanley J Korsmeyer. Cell death: critical control points. *Cell*, 116(2):205– 219, 2004.
82. GA Arteca, FM Fern´andez, EA Castro, GA Arteca, FM Fern´andez, and EA Castro. Rayleigh-schrodinger perturbation theory (rspt). *Large Order Perturbation Theory and Summation Methods in Quantum Mechanics*, pages 45–71, 1990.
83. Chr Møller and Milton S Plesset. Note on an approximation treatment for many-electron systems. *Physical review*, 46(7):618, 1934.
84. Christopher W Murray, Gregory J Laming, Nicholas C Handy, and Roger D Amos. Kohn—sham bond lengths and frequencies calculated with accurate quadrature and large basis sets. *Chemical physics letters*, 199(6):551–556, 1992.
85. Daniel Finkelstein-Shapiro, Stephen K Davidowski, Paul B Lee, Chengchen Guo, Gregory P Holland, Tijana Rajh, Kimberly A Gray, Jeffery L Yarger, and Monica Calatayud. Direct evidence of chelated geometry of catechol on tio2 by a combined solid-state nmr and dft study. *The Journal of Physical Chemistry C*, 120(41):23625–23630, 2016.
86. Robert B Murphy, Michael D Beachy, Richard A Friesner, and Murco N Ringnalda. Pseu-dospectral localised mo/ller–plesset methods: Theory and calculation of conformational ener-gies. *The Journal of chemical physics*, 103(4):1481–1490, 1995.
87. Seiji Tsuzuki and Hans P L¨uthi. Interaction energies of van der waals and hydrogen bonded systems calculated using density functional theory: Assessing the pw91 model. *The Journal of Chemical Physics*, 114(9):3949–3957, 2001.
88. Seiji Tsuzuki, Tadafumi Uchimaru, and Kazutoshi Tanabe. Intermolecular interaction poten-tials of methane and ethylene dimers calculated with the møller–plesset, coupled cluster and density functional methods. *Chemical physics letters*, 287(1-2):202–208, 1998.
89. John P Perdew, Kieron Burke, and Matthias Ernzerhof. Generalised gradient approximation made simple. *Physical review letters*, 77(18):3865, 1996.
90. Javier Carmona-Esp´ındola, Jos´e L G´azquez, Alberto Vela, and SB Trickey. Generalised gra-dient approximation exchange energy functional with correct asymptotic behavior of the cor-responding potential. *The Journal of Chemical Physics*, 142(5), 2015.
91. Benjamin G Janesko. Rung 3.5 density functionals: Another step on jacob's ladder. *Interna-tional Journal of Quantum Chemistry*, 113(2):83–88, 2013.
92. Frank Jensen. *Introduction to computational chemistry*. John wiley & sons, 2017.
93. A Bende, A Vibok, GJ Halasz, and S Suhai. Bsse-free description of the formamide dimers. *International Journal of Quantum Chemistry*, 84(6):617–622, 2001.
94. D Moncrieff and S Wilson. A universal basis set for high-precision molecular electronic struc-ture studies: correlation effects in the ground states of, co, bf and. *Journal of Physics B: Atomic, Molecular and Optical Physics*, 31(17):3819, 1998.
95. Ugurlu, S.Y., McDonald, D., & He, S. (2024). MEF-AlloSite: An accurate and robust Multimodel Ensemble Feature selection for the Allosteric Site identification model. Journal of Cheminformatics, 16(1), 116.
96. Ugurlu, S.Y., et al. (2024). Cobdock: An accurate and practical machine learning-based consensus blind docking method. Journal of Cheminformatics, 16(1), 5.
97. Schmidt, A., Simonovic, S., Kalenius, E., Nissinen, M., & Rissanen, K. (2016). Supramolecular exo-functionalized palladium cages: fluorescent properties and biological activity. Dalton Transactions, 45(20), 8556–8565.
98. Duan, X., et al. "Nanoparticle formulations of cisplatin for cancer therapy." Wiley Interdisciplinary Reviews: Nanomedicine and Nanobiotechnology, 8(5):776-791, 2016.
99. Boulikas, T. "Molecular mechanisms of cisplatin and its liposomally encapsulated form, Lipoplatin™. Lipoplatin™ as a chemotherapy and antiangiogenesis drug." Cancer Therapy, 5:351-376, 2007.
100. Pourmadadi, M., et al. "Cisplatin-loaded nanoformulations for cancer therapy: A comprehensive review." Journal of Drug Delivery Science and Technology, 77:103928, 2022.
101. Li, X., et al. "Superior antitumor efficiency of cisplatin-loaded nanoparticles by intratumoral delivery with decreased tumor metabolism rate." European Journal of Pharmaceutics and Biopharmaceutics, 70(3):726-734, 2008.
102. Jang, B., et al. "Dual delivery of biological therapeutics for multimodal and synergistic cancer therapies." Advanced Drug Delivery Reviews, 98:113-133, 2016.
103. Dai, W., et al. "Combination antitumor therapy with targeted dual-nanomedicines." Advanced Drug Delivery Reviews, 115:23-45, 2017.
104. Gurunathan, S., et al. "Nanoparticle-mediated combination therapy: two-in-one approach for cancer." International Journal of Molecular Sciences, 19(10):3264, 2018.

7. Supporting information

The supporting information provides additional details and data that complement the main findings of this study on the investigation of metallacages for cisplatin encapsulation using DFT simulations. This section includes fundamental background information on metallacages, their relevance in drug delivery systems, and the theoretical framework employed in our DFT simulations. Furthermore, it presents supplementary experimental results, computational data, and analyses that support the primary conclusions of the research. By offering these additional insights and data, we aim to enhance the understanding of the encapsulation mechanisms and validate the accuracy and robustness of our theoretical predictions.

7.1 Background Theory

Computational chemistry is almost a new branch compared to classical chemistry approaches. On the other hand, several unrealistic possibilities can be eliminated using computational methods and computational chemistry approaches. The already discussed plans can lead to a deep understanding of systems and suggest novel strategies to overcome the current limitations, such as the high toxicity of the anti-cancer Pt (II) compound cisplatin. The benefits of using theory and models are that they eliminate vague or contradictory results and reasons, optimise processes and experiments, and predict future works. It is also available for a complex or hazardous to find using the experiment and to boost success probability, saving time [57].

Ab initio quantum chemistry based on QM (Quantum Mechanics) principles has played a crucial role in comprehending and modelling atoms and molecules. John Pople and Walter Kohn were awarded The Nobel Prize in 1998 thanks to their success in theoretical chemistry [76]. Following DFT, the convention ab initio wave function became the second most exciting approach since DTF uses 4N variables (three spatial and one spin variable for each of the N electrons) to solve the Schrodinger equation [66]. Also, a model uses the electronic Schrodinger equation to calculate by considering the electron density, the position of electrons, and the particle energy level, called model chemistry [66]. The Hamiltonian is just a mathematical description of the operation [77]. The description of the system using the equation is challenging since the equation has various variables based on the probability of several statuses. Therefore, even if the supercomputers making the quantum calculation have millions and millions of lines of code to increase accuracy, it is not fast enough to explain and model every existing system. The number of possibilities is almost infinite; therefore, scientists have spent time finding a mathematical algorithm to decrease computational work as well as the time of the process [76]. To solve the equation, we need to describe the wave function based on the wave function of the hydrogenic atom since it is the only solution to the Schrodinger equation. Therefore, predicting imaginary wave function and calculation Hamiltonian becomes clear on one side of the equation; only if the wave function is actual this equation is correct [78].

Quantum Chemical Theories

In a quantum system, an electron world is compared with a classical system like the solar system or a habitat; almost every physical law has to be changed. It became clear after that double-slit diffraction plays a crucial role in quantum mechanics. The electron diffraction is shown using ion beam (FIB) milled nanoslits, and it is discussed that the phenomena of wave-particle duality demonstrate that all particles have not only wave but particle properties via double-slit diffraction [79, 80, 81]. The wave function exhibiting features of community electrons instead of individual electron systems was proven after these experiments. Therefore, wave function (symbolised as ψ) is statistical data from a group of quantum mechanics, so it is inappropriate to apply to a sole system. It is a function based on complex-valued likelihood amplitude. It is not impossible to forecast the location of the coordinates of particles or an electron or the momenta of all the particles.

There are two highly efficient approaches: wave function-based approaches and DFT for the electronic Schrodinger equation, the time evolution of quantum wave packets. Firstly, Slater determinants are the critical point for wave function-based methods and can be used to optimise the coefficients and orbitals. The other technique is the Moller-Plesset perturbation theory, which is a quantum chemistry method having electron exchange impacts, and it is based on Rayleigh-Schrodinger perturbation theory (RS-PT) [76, 82, 83]. They have several pros and cons based on the system property, such as the number of elections, exchange-energy correlation, and electron position.

DFT, the least expensive method, covers the second theoretical approach based on the Hohenberg-Kohn theorem via an electron density function [76]. However, finding an incredibly accurate energy function has taken more than 20 years, and the accuracy has improved; it cannot be neglected that limitations and uncertainty still exist [76]. It can correctly describe the periodic table elements' equilibrium geometries and the investigation of conformational and hydrogen bond interactions [76, 84, 85]. On the other hand, it does not have high prediction power about energy alteration coming from the bond formation, breaking the bond, and the other molecular interaction when compared to MP2 (second-order Moller-Plesset perturbation), with some exceptional cases [86, 87]. The other limitation of the approach is the van der Waals interaction [88], yet MP2 can overcome the problem [86, 87]. DFT is best for explaining medium to extensive systems [88]. On the other hand, DTF is inferior to MP2 when non-bonded interaction from the small to the comprehensive system is the point [88].

Kohn-Sham DFT is used to identify a fictitious system of non-interacting particles. Several methods have been tested and developed to model the exchange-correlation energy. The most straightforward approach is the local spin density (LSD), which yields enough accuracy for equilibrium geometries, lattice constants, vibrational frequencies, and bulk moduli [66]. The generalised gradient approximation (GGA) can explain energy barriers, structural energy differences, and total energies rather than LSD. Semiempirical GGA's are incredibly suitable for small molecules, yet they cannot be used to delocalize the uniform gas or model electrons in metals [89]. The Perdew-Burke-Ernzerhof (PBE) function for exchange-energy correlation is a member of the generalised gradient approximation (GGA) [90].

The schematic picture of exchange-correlation functionals demonstrates the relationship between theories with their efficiency and simplicity according to each other. Therefore, the exchange-correlation (XC) functionals must balance cost and accuracy. The first three steps are semilocal, and the others are a nonlocal exchange-correlation function [91].

A basis set referring to the set of (nonorthogonal) one-particle functions is used to determine the wave function and to express the unknown molecular orbitals (MOs) using a set of known functions [54]. It can be identified that an unknown MO is a function in endless space defined by a completed basis set by assuming the centre on the nuclei [54]. It is beneficial to determine other features of a molecule, such as a dipole moment, polarisability electron density, spin density, and chemical shifts; in other words, a model calculates molecular orbitals (MOs) using the Linear Combination of Atomic Orbitals (LCAO) approximation. On the other hand, a scientist has to identify molecular geometry, basis set, and type of calculation for exchange-correlation energy in the computer program having codes to calculate wave function and the features of a molecule. Therefore, selecting a basis set is a critical choice for the calculation, so several points exist to choose the correct basis set for a system. First, a basis set has been appropriate for the structure, making the program faster [54]. For example, a more extensive basis set, such as LanL2DZ, is not an excellent choice for a small organic compound. The other significant point in selecting a basis set is that it makes calculation easy [54]. In other words, a basis set yields chemically meaningful results, and the cost is the other factor affecting the selection of a basis set [54]. Besides, not all basis sets have data about each periodic table element, so when choosing a basis set, it must have figures about atoms in the structure [54]. In addition, the basis set and the degree of electron correlation impact the accuracy, cost, and time. Therefore, the trade-off is the most vital factor for picking a basis set having balanced accuracy, process time, and computational cost. The point that needs to be considered during the selection of the basis set is diffuse functions, which negatively affect the accuracy of the calculation. The basis set must be appropriate to reach convergence regarding electric energy [54].

There are three main types of orbitals. One of the basis sets is hydrogen-like orbitals, which are derived for one electron atom, so they are unsuitable for many electron atoms.

It yields the absolute explanations for the hydrogen atom. It cannot be used for a complex system even if it is mutually orthogonal as an advantage. As for the Slater-type orbitals (STOs), several STOs are combined to symbolise each HF orbital [92]. It has also been completed and set to be used for several calculations. Yet, it is not reciprocally orthogonal and a time saver because of an increasing number of functions, and there is no node as a weak point. Therefore, nodes can be determined by combining the STOs as a straight line. Besides, it highly reflects the orbitals for the hydrogen.

Using Slater-Type Orbitals (STOs) in semi-empirical methods provides higher accuracy but requires more computational time. This issue can be addressed by linearly combining Gaussian-Type Orbitals (GTOs) to approximate the STOs, resulting in what is known as "STO-nG" basis sets. STOs can also be employed in density functional theory (DFT) calculations. The STO-3G basis set, a minimum basis set, is the most commonly used, but it may not be ideal due to its size limitations [54]. In general, larger basis sets tend to provide better results than smaller ones. Other standard basis sets of this type include STO-4G and STO-6G.

The third basis set is Gaussian-type orbitals (GTOs), having been completed. The completed means that endless functions must be utilised [54]. An uncompleted or an infinite basis set can express the part of the coordinate axes of MOs [54]. Therefore, the smaller basis set is weak, providing a poor system description. It is much faster because of the determined vibrational coefficient when compared to Gaussian and others, yet it is not reciprocally orthogonal, either. Linear combinations of GTOs can be utilised to approximate STOs. A just GTO basis function is not as satisfactory as an STO; combined, several GTOs in a direct line have been improved and become more satisfying. The other group for the basis set is minimal basis sets, represented by STO-NG (N is the number of GTOs utilised). The main difference between GTOs and STOs is that the variable ”r” in the exponential function is squared for GTOs. Also, combinations of them can yield knowledge about a system. A favourable example is joining three d-type Cartesian GTOs, which generate a Cartesian GTO of s-type [93]. GTOs are inferior to STOs in three cases: to explain electrons located near the nucleus, zero slopes at the nucleus, and to represent “tail” electron behaviour with less accuracy [92].

We can categorise basis sets as a minimum basis set, double zeta type basis, triple zeta (TZ), quadruple zeta (QZ) and quintuple or pentuple zeta (PZ or 5Z, but not QZ).

Table 11: Categorisation and Characteristics of Basis Sets Used in Computational Chemistry.

Basis Set	Features
Minimum Basis Set	One basis function for atomic orbitals (AO).
	Convenient for all electrons of the neutral atoms.
	Fast calculation.
	The shape of all orbitals is the same, which is not true.
Double Zeta (DZ)	Considers bonding in a molecule, e.g., an H-C bond is calculated.
	Much better description than the minimum basis set.
	Propagates a split valence basis.
	Treats each orbital separately.
	Two basis functions per valence AO, called a valence double zeta basis set.
	Example: 3-21G, 6-31G, cc-pVDZ.
Triple Zeta (TZ)	Three times as many functions as a minimum basis set, e.g., three p-functions for hydrogen.
	Creates a triple split valence basis set.
	Three basis functions per valence AO, called a valence triple zeta basis set.
	Example: 6-311G, cc-pVTZ.
Quadruple Zeta (QZ) and Quintuple Zeta (5Z)	The next level basis sets.

This table summarises various basis sets, including the minimum basis set, double zeta, triple zeta, quadruple zeta, and quintuple zeta. Each category is characterised by the number of basis functions per atomic orbital (AO), the accuracy of the molecular bonding description, and specific examples of basis sets used in DFT and other quantum chemical calculations. The progression from the minimum to the quintuple zeta basis set reflects increased computational complexity and accuracy.

The other basis set order is that Minimal < Split Valence < Polarized < Diffuse according to an appropriate approximation to the actual wave function. The number of primitives used affects the accuracy of energy calculation [94]. The energy decreases by increasing the number of primitives benefitting from the calculation.65 The other issue about the basis set is the polarization basis function, based on the interaction of the neighbouring nuclei. The interaction can distort orbitals; therefore, flexible shapes must be calculated correctly. Polarisation functions have to be added into a basis set to increase accuracy. The other function to augment accuracy is a diffuse function, used to clarify anions, excited states, and very electronegative atoms such as fluorine. It is also significant in accurately describing polarizabilities or binding energies of van der Waals. An example of combining these functions to a basis set is aug-cc-pVXZ. For instance, ‘cc’ means “correlation consistent”, ‘p’ means “polarisation functions added”, and ‘aug’ means “augmented” with (essentially) diffuse functions [94].

Gassian software background

There are several semi-empirical methods in Gaussian 9 software. The most common semi-empirical quantum chemistry is Neglect of Diatomic Differential Overlap, Complete Neglect of Differential Overlap (CNO), and Intermediate Differential Overlap (INDO, MINDO) [54, 55]. They are in the Zero Differential Overlap (ZDO) method group, disregarding all two-electron integrals [54, 55]. A semi-empirical model benefits results and approximations from experiments to improve the model's performance [56]. Most semi-empirical methods benefit only the s- and p-orbitals with Staler-type orbitals [57]. The other advantages of semi-empirical methods are that they are inexpensive and time-saving. They have pre-calculated data as a part of the program, which can guide them in solving the Schrodinger equation. Semi-empirical methods are better for a prominent structure with more than 1000 atoms [58]. The local density function, Hartree Fock, results in better accuracy for a 100-atom system [59]. The Hartree-Fock model forms the foundation of semi-empirical methods, which assume only valence electrons. The engine employs GTOs, enabling the application of molecular mechanics, semi-empirical methods, the Hartree-Fock model, post-Hartree-Fock methods, DFT, and molecular modelling [60].

To enhance the accuracy of our calculations and improve predictive capabilities while optimising both time and financial resources, we have selected semi-empirical methods that integrate the strengths of Hartree-Fock (HF) and the Perdew-Burke-Ernzerhof (PBE) functionals. Specifically, we will employ PBE0 and HF as the theoretical framework and LanL2DZ as the basis set. This approach balances computational efficiency with the reliability of results, making it an ideal choice for complex molecular systems where precision is paramount. By leveraging these methods, we aim to achieve a high level of accuracy without compromising on computational expediency.

Gaussian software provides a robust platform for implementing semi-empirical quantum chemistry methods, such as Neglect of Diatomic Differential Overlap (NDDO), Complete Neglect of Differential Overlap (CNDO), and Intermediate Neglect of Differential Overlap (INDO, MINDO). These approaches fall under the Zero Differential Overlap (ZDO) category, streamlining calculations by neglecting all two-electron integrals. By leveraging experimental data to enhance predictive capabilities, semi-empirical models improve efficiency without compromising accuracy. These methods typically focus

on s- and p-orbitals and use Slater-type basis functions for computational simplicity. Their primary advantages include affordability, speed, and the ability to handle larger molecular systems. For systems with more than 1000 atoms, semi-empirical approaches are ideal, while more computationally demanding methods like Hartree-Fock are better suited for smaller systems. The Gaussian suite supports a wide range of computational techniques, from molecular mechanics and semi-empirical methods to DFT and post-Hartree-Fock models, making it a versatile tool for various applications.

Hartree-fock background

Using a single Slater determinant or a single permanent N-spin orbital, the Hartree-Fock (HF) method, a vibrational, wave function-based approach, determines the wave function of a system [45, 46, 47]. The core principle of HF involves calculating a vibrational wave function for single-particle orbitals. However, as the number of electrons in the system rises, so does the computational difficulty of figuring out the wave function [46]. The Born-Oppenheimer approximation has been mainly used to manage this complexity, simplifying the problem by separating nuclear and electronic motion. By treating the electronic degrees of freedom separately, this approximation reduces the computational burden, enabling more manageable calculations even as the number of electrons increases [47]. Consequently, Hartree-Fock theory, as a mean-field approach, provides a solution for many cases, making it the most straightforward wave function-based method.

The Hartree-Fock (HF) method calculates the wave function of a multi-electron system using a mean-field approximation, where electrons interact with an average potential created by all other electrons. Employing a single Slater determinant, HF simplifies the inherently complex multi-electron problem. The computational cost increases significantly with the number of electrons, making the Born-Oppenheimer approximation essential to separate nuclear and electronic motions, thereby reducing complexity. While HF offers a foundational wave-function-based approach, its limitations stem from the mean-field assumption, which does not account for electron correlation. Nonetheless, it remains a cornerstone of quantum chemistry and serves as a starting point for more advanced methods. Its combination of accuracy and computational feasibility makes HF suitable for small to medium-sized systems and a critical component of many hybrid and semi-empirical models.

PBE and PBE0 background:

PBE, while computationally efficient, has limited performance in specific applications [68]. Fortunately, hybrid functionals incorporating Hartree-Fock (HF) exchange can improve accuracy and performance compared to PBE [66]. Hybrid functionals combine non-local Hartree-Fock exchange with local or semi-local DFT/GGA exchange [69]. These hybrid functionals aim to enhance the calculation's accuracy while reducing computational costs and time. Hybrid functions can mitigate these errors, offering more accurate descriptions of thermochemical properties such as surface energies, ionisation potentials, and lattice constants [56]. For instance, the mean absolute errors (MAE) associated with PBE are significantly larger—nearly three times—than those found in hybrid functionals [70]. By incorporating the Hartree-Fock exchange, hybrid functions can improve the accuracy of band gap predictions [71]. Consequently, a hybrid function like PBE0 has been employed to investigate cisplatin encapsulation because it combines the accuracy of Hartree-Fock exchange with the efficiency of DFT.

PBE0 is a prominent example of a hybrid function that combines the PBE exchange-correlation with the Hartree-Fock exchange in a 3:1 ratio. This method blends the strengths of both approaches, leading to better predictions of bond lengths, electron distributions, vibrational frequencies, and atomisation energies. The hybridisation of Hartree-Fock and PBE makes PBE0 particularly well-suited for calculating the properties of various molecules with a high degree of accuracy [71]. The specific system and property under study should guide the choice between PBE, Hartree-Fock, and hybrid functionals like PBE0 despite the challenge of determining a universally superior method. In many cases, PBE0's balanced approach makes it a reliable choice for various chemical systems.

The Perdew-Burke-Ernzerhof (PBE) functional is a widely used Generalized Gradient Approximation (GGA) method in Density Functional Theory (DFT) due to its computational efficiency and reasonable accuracy for many systems. However, its performance can be limited in cases requiring high precision, such as predicting band gaps or thermodynamic properties. Hybrid functionals, such as PBE0, address these shortcomings by integrating a fraction of Hartree-Fock exchange with PBE's exchange-correlation energy. PBE0, with its balanced 3:1 ratio of PBE to HF exchange, achieves improved accuracy in bond lengths, vibrational frequencies, and electronic properties. Hybrid methods like PBE0 are particularly effective for systems requiring a balance between computational efficiency and predictive reliability, making them ideal for studying the intricate details of molecular systems like metallacages.

LanL2DZ background

LanL2DZ is implemented using the Gen and GenECP keywords in Gaussian 09 software. For example, it describes the valence orbitals of ruthenium by considering 28 core electrons (1s2 2s2 2p6 3s2 3p6 3d10 = Argon) and utilising a 3s3p2d basis set. LanL2DZ is suitable for transition metals and other elements, making it a valuable basis set for investigating metallacages [65]. Additionally, due to its improved accuracy, researchers generally prefer DFT over the Hartree-Fock (HF) method for predicting atomic behaviour and molecular properties [54]. Researchers can also use available codes to create hybrid basis sets, enhancing existing ones by combining various methods.

The core (inner) electrons do not directly impact chemical bond formation, which is a fundamental concept in the development of Effective Core Potential (ECP) Basis Sets [74]. This approach uses an average potential profile to describe the core electrons, as detailing each electron is computationally expensive [75]. LanL2DZ, an ECP basis set, was developed to reduce computational costs associated with metal-based structures and to account for relativistic effects in deep core electrons [65]. Although LanL2DZ provides high accuracy for elements such as sodium (Na) and heavier atoms, it lacks polarisation functions, which are crucial for accurately describing frontier orbitals, redox reactions, and electronic excitations. Also, some ECPs do not include diffuse functions necessary for effectively describing anions. Including d-type polarisation functions can enhance the accuracy of the basis set. While

Several ECP basis sets are available, such as Def2TZVPP, Def2SVP, and SDD, valence triple-ζ (triple zeta) functions can significantly increase computational costs [65]. Thus, LanL2DZ remains a practical and efficient choice for investigating metallacage structures.

LanL2DZ, a popular basis set in quantum chemistry, is frequently used for transition metals and heavier elements due to its efficiency and versatility. It employs Effective Core Potentials (ECPs) to represent core electrons, reducing computational demands by focusing on valence electron interactions. LanL2DZ is particularly useful for large metal-containing systems, as it incorporates relativistic effects while maintaining manageable computational costs. However, its lack of polarisation functions can limit accuracy in describing electronic excitations, redox reactions, or anionic systems. These limitations can be mitigated by augmenting LanL2DZ with additional functions or by combining it with other basis sets tailored for specific needs. Despite alternatives like Def2SVP or SDD offering higher precision, the practical balance of efficiency and accuracy makes LanL2DZ a widely adopted choice for investigating metal-organic structures, including metallacages.